इंटरनेट मानक

Disclosure to Promote the Right To Information

Whereas the Parliament of India has set out to provide a practical regime of right to information for citizens to secure access to information under the control of public authorities, in order to promote transparency and accountability in the working of every public authority, and whereas the attached publication of the Bureau of Indian Standards is of particular interest to the public, particularly disadvantaged communities and those engaged in the pursuit of education and knowledge, the attached public safety standard is made available to promote the timely dissemination of this information in an accurate manner to the public.

“जानने का अधिकार, जीने का अधिकार”
Mazdoor Kisan Shakti Sangathan
“The Right to Information, The Right to Live”

“पुराने को छोड नये के तरफ”
Jawaharlal Nehru
“Step Out From the Old to the New”

IS 12737 (1988): Standard Test Procedures for Semiconductor X-Ray Energy Spectrometers [LITD 8: Electronic Measuring Instruments, Systems and Accessories]

“ज्ञान से एक नये भारत का निर्माण”
Satyanarayan Gangaram Pitroda
“Invent a New India Using Knowledge”

Act Number 22 of 2005
The Indian Parliament
RIGHT TO INFORMATION

Made Available By
Public.Resource.Org

“ज्ञान एक ऐसा खजाना है जो कभी चुराया नहीं जा सकता है”
Bhartṛhari—Nītiśatakam
“Knowledge is such a treasure which cannot be stolen”

BLANK PAGE

BRUTUM FULMEN
IGNORANTIA JURIS NON EXCUSAT
PROTECTED BY COPYRIGHT

IS 12737 : 1988
IEC Pub 759 (1983)

Indian Standard (Reaffirmed 2006)

STANDARD TEST PROCEDURES FOR SEMICONDUCTOR X-RAY ENERGY SPECTROMETERS

UDC 621·384·8

© BIS 1990

BUREAU OF INDIAN STANDARDS
MANAK BHAVAN, 9 BAHADUR SHAH ZAFAR MARG
NEW DELHI 110002

February 1990

Price Group 14

Indian Standard

STANDARD TEST PROCEDURES FOR SEMICONDUCTOR X-RAY ENERGY SPECTROMETERS

NATIONAL FOREWORD

This Indian Standard, which is identical with IEC Pub 759 (1983) 'Standard test procedures for semiconductor X-ray energy spectrometers' issued by the International Electrotechnical Commission (IEC), was adopted by the Bureau of Indian Standards on 21 September 1988 on the recommendation of the Nuclear Instrumentation Sectional Committee (LTDC 26) and approval of the Electronics and Telecommunication Division Council.

Wherever the words 'International Standard' appear, reefrring to this standard, they should be read as 'Indian Standard'.

Comma (,) has been used as a decimal marker in the adopted standard while in Indian Standard, the current practice is to use point (.) as the decimal marker.

CROSS REFERENCES

In this standard the following International Standards are referred to. Read in their respective places the following :

International Standard	*Corresponding Indian Standard*	*Degree of Correspondence*
IEC Pub 50 International Electrotechnical Vocabulary (IEV)	IS 1885 (Part 63) : 1985 Electrotechnical vocabulary: Part 63 Nuclear instrumentation	Identical
IEC Pub 333 Test procedures for semiconductor detectors for ionizing radiation	IS 11425 : 1985 Test procedure for semiconductor charged-particle detectors	Identical
IEC Pub 340 Test procedures for amplifiers and preamplifiers for semiconductor detectors for ionizing radiation	IS 11645 : 1985 Test procedures for amplifiers and preamplifiers for semiconductor detectors for ionizing radiation	Identical
IEC Pub 656 Test procedures for high-purity germanium detectors for X and gamma radiation	IS 12639 : 1988 Test procedures for high-purity germanium detectors for X and gamma radiation	Identical

Only the English language text of the International Standard has been retained while adopting it in this Indian Standards.

As in the Original Standard, this Page is Intentionally Left Blank

1. Scope

This standard presents standard test procedures for semiconductor X-ray energy spectrometers. Such systems consist of a semiconductor radiation detector assembly and signal processing electronics interfaced to a pulse-height analyzer/computer. Test procedures for pulse-height analyzers and computers are not covered in this standard. Clause 5 is essentially tutorial.

2. Object

This standard is not intended to imply that all tests described herein are mandatory, but only that such tests as are carried out shall be performed in accordance with the procedures described herein.

Companion publications to this standard are IEC Publication 333: Test Procedures for Semiconductor Detectors for Ionizing Radiation, IEC Publication 340: Test Procedures for Amplifiers and Preamplifiers for Semiconductor Detectors for Ionizing Radiation, and IEC Publication 656: Test Procedures for High-purity Germanium Detectors for X and Gamma Radiation. The list of symbols and the glossary are derived from those in the above-mentioned publications.

Contrary to previous convention in the X-ray spectroscopy field, this standard utilizes the characteristic energy E of the X-ray rather than its wavelength λ. This approach is consistent with the fact that the basic quantity measured by this type of spectrometer is the X-ray energy. A convenient conversion is provided by the relationship:

$$\lambda\,(\mathrm{m}) = 12.4 \cdot 10^{-10}\, E^{-1}\ (\mathrm{keV})$$

$$(\lambda\,(\text{Å}) = 12.4 \cdot E^{-1}\ (\mathrm{keV}))$$

3. Glossary (according to English alphabetical order)

Analog to digital converter (ADC)

A sub-assembly designed to provide an output signal which is a digital representation of the analog input signal (IEV 391-11-36).

Background (associated with a spectral peak from a semiconductor detector)

Non-ideal spectral response which results from radiation which is not a part of the monoenergetic line of interest.

Baseline (at pulse peak)

The instantaneous value that the voltage would have had at the time of the pulse peak in the absence of that pulse (IEC Publication 340).

Baseline restoration (BLR)

Appropriate linear or non-linear techniques which are used to accelerate the return of a voltage to its baseline.

Bias resistor (of a semiconductor radiation detector)

The resistor through which bias voltage is applied to the detector (IEC Publication 340).

Biased pulse amplifier

A pulse amplifier designed to provide an amplified output pulse only for that portion of an input signal exceeding a predetermined threshold value (IEV 391-11-05).

Bias voltage (of a semiconductor radiation detector)

The voltage applied to the detector to produce the electric field to collect the signal charge.

Breakdown (of a reverse-biased junction)

Transition from a state of high dynamic resistance to a state of substantially lower dynamic resistance for increasing magnitude of reverse voltage (IEV 391-10-50).

Breakdown region (of a semiconductor diode characteristic)

That entire region of the voltage-current characteristic beyond the initiation of breakdown for increasing magnitude of reverse current.

Breakdown voltage (of a semiconductor diode)

The voltage measured at a specified current in the breakdown region

Capacitance (of a semiconductor radiation detector)

The small-signal capacitance measured between terminals of the detector under specified conditions of bias and frequency.

Charge carrier (abbreviation: carrier)

In a semiconductor, a free conduction electron or a mobile hole (IEV 391-10-53).

Charge collection time (of a semiconductor detector)

By convention, the time interval for the integrated current due to the charge collected in the semiconductor detector, after the passage of an ionizing particle, to increase from 10% to 90% of its final value (IEV 391-10-59).

Clip, clipping (jargon)

A limiting operation such as: 1) use of a high-pass filter (see Differentiated), or 2) a non-linear operation such as diode limiting of pulse amplitude.

Compensated semiconductor

A semiconductor in which the effects of the impurities of a given type on the charge carrier density partially or completely cancel those of the other type. Such a semiconductor has properties which are similar to those of an intrinsic semiconductor (IEV 391-05-03).

Compensated semiconductor detector

A semiconductor detector consisting of a region of compensated semiconductor between a P-type region and an N-type region (IEV 391-09-44).

CR-RC shaping

The pulse shaping present in an amplifier that has a simple high-pass filter consisting of a capacitor and a resistor together with a simple, low-pass filter, separated by impedance isolation. Pulse shaping in such an amplifier cuts off at 6 decibels per octave at both ends of the band.

Crest factor (of an average reading or root-mean-square voltmeter)

The ratio of (1) the peak voltage value that an average reading or root-mean-square voltmeter will accept without overloading to (2) the full scale value of the range being used for measurement (IEC Publication 340).

D.C. level (see *Baseline*)

Dead layer (of a semiconductor detector)

A layer of a semiconductor detector in which no significant part of the energy lost by particles can contribute to the resulting signal (IEV 391-10-55).

Decay time constant

The time for a true single-exponential waveform to decay to a value of $1/e$ of the original height (IEC Publication 340).

Depletion layer (in a semiconductor detector)

A layer of a semiconductor detector in which no significant part of the energy lost by particles can contribute to the resulting signal.

Differentiated (pulse) (pulse amplifier jargon)

A pulse that is passed through a high-pass network, such as a CR filter (IEC Publication 340).

Efficiency (of a semiconductor radiation detector for a monoenergetic radiation source)

The ratio of the number of events in the spectral distribution to the total number of photons incident on the active detector volume during the same time interval.

Energy resolution (FWHM) (of a semiconductor radiation detector)

The detector's contribution (including detector leakage current noise), expressed in units of energy, to the FWHM of a pulse-height distribution corresponding to an energy spectrum (IEC Publication 340).

Energy resolution (per cent) (of a semiconductor radiation detector)

One hundred times the energy resolution divided by the energy for which the resolution is specified (IEC Publication 340).

Equivalent noise referred to input (of a linear amplifier)

The value of noise at the input that would produce the same value of noise at the output as does the actual noise source (IEC Publication 340).

Full energy peak (for a monoenergetic photon spectrum for a semiconductor spectrometer system)

The distribution of events within the peak of the pulse-height distribution spectrum representing response to the monoenergetic photon source.

Note — Notwithstanding other definitions or procedures for subtracting background and other distortions, the full energy peak intensity is defined as not including any events which exceed a Gaussian distribution by more than a factor 2σ.

Full energy peak efficiency (of a semiconductor radiation detector)

The ratio of the number of events in the full energy peak of the spectral distribution to the total number of photons incident on the active detector volume during the same time interval.

Full width at fifth maximum

Same as full width at half maximum except that measurement is made at one-fifth of the maximum ordinate rather than one-half (N.B.: This definition should be written in its entirety).

Full width at half maximum (FWHM)

In a distribution curve comprising a single peak, the distance between the abscissae of two points on the curve whose ordinates are half of the ordinate of the peak.

Note. — If the curve considered comprises several peaks, a full width at half maximum exists for each peak (IEV 391-15-08).

Full width at tenth maximum (FWTM)

Same as full width at half maximum except that measurement is made at one-tenth of the maximum ordinate rather than one-half (IEC Publication 340).

FWFM (see *Full width at fifth maximum*)

FWHM (see *Full width at half maximum*)

FWTM (see *Full width at tenth maximum*)

Gate

A device or element that, depending upon one or more specified inputs, has the ability to permit or inhibit the passage of a signal.

Geometry, detector (detector jargon)

The physical configuration of a solid-state detector.

Inactive region (of a semiconductor radiation detector)

A region of a detector in which charge created by ionizing radiation does not contribute significantly to the signal (IEC Publication 340).

Integral non-linearity (INL) (%)

The departure from the linear response expressed as a percentage of the maximum rated output pulse amplitude (IEC Publication 340).

Integrated (pulse) (pulse amplifier jargon)

A pulse that is passed through a low-pass network, such as a single RC network or a cascaded RC network (IEC Publication 340).

Integrating preamplifier

A pulse preamplifier in which individual pulses are intentionally integrated by passive or active circuits (IEC Publication 340).

Intrinsic semiconductor (I-type)

An effectively pure semiconductor in which, under conditions of thermal equilibrium, the charge carrier densities of each sign are nearly equal (IEV 391-05-02).

Note. — By extension, this term is incorrectly used to designate compensated semiconductors.

Inversion layer

For a given type of semiconductor, a surface layer of the opposite type (IEV 391-10-57).

Ionization detector

A radiation detector based on the use of ionization in the sensitive volume of the detector (IEV 391-08-06).

Junction (of a semiconductor radiation detector)

A transition layer between semiconductor regions of different electrical properties, or between a semiconductor and a superficial layer of different type. This layer is characterized by a potential barrier impeding the movement of charge carriers from one region to the other (IEV 391-10-42) (IEC Publication 340).

Junction depth (of a p-n semiconductor radiation detector)

The distance below the crystal surface at which the conductivity type changes.

Leakage current (of a semiconductor radiation detector)

The total detector current flowing at the operating bias in the absence of radiation.

Linear gate

A gate whose presence does not affect the linearity of the gated signal.

Line-to-background ratio (of a spectral line)

The ratio of the intensity of a monoenergetic line to the intensity of the background immediately adjacent to the line.

Lithium drifted semiconductor detector

A compensated semiconductor detector in which the compensated region is obtained by causing lithium ions to move through a P-type crystal under an applied electric field in such a way as to compensate the charge of the bound impurities (IEV 391-09-45).

Load impedance (of a semiconductor radiation detector)

The impedance shunting the detector, and across which the detector output voltage signal is developed (IEC Publication 340).

Load resistance (of a semiconductor radiation detector)

The resistive component of the load impedance (IEC Publication 340).

Modal channel

The modal channel is that channel in the distribution containing the largest number of counts.

Multichannel analyzer (MCA)

An analyzer with more than one channel, usually containing a sufficient number of channels to determine a distribution function of a group of signals by sorting the pulses into the various channels according to one of their characteristics (amplitude, duration, etc.) (IEV 391-11-32).

Noise linewidth

The contribution of noise to the width of a spectral peak.

Non-injecting contact (of a semiconductor radiation detector)

A contact at which the carrier density in the adjacent semiconductor material is not changed from its equilibrium value (IEC Publication 340).

Non-linearity (of a pulse amplifying system)

Distortion caused by a deviation from a desired linear relationship between specified measures of the ouptut and input pulse amplitudes of a system or device.

Ohmic contact (of a semiconductor radiation detector)

A purely resistive contact, i.e. one that has a linear voltage-current characteristic throughout its entire operating range (IEC Publication 340).

Overload pulse

Any signal which drives a section of the amplifying chain into saturation.

Paralyzable system

Any system or device whose response characteristics contain a region where the ratio of output to input count rate decreases with increasing input count rate.

Partially dead region or layer (of a semiconductor detector)

Any region or layer on or in the detector which contributes an output pulse which is less than the full energy peak for that incident radiation.

Per cent energy resolution (see *Energy resolution [per cent]*)

Pile-up (in a counting assembly)

A phenomenon where a pulse occurs on the tail of the preceding pulse so as to result in an incorrect indication of the pulse amplitude. The pile-up can also result in failure to resolve some pulses (IEV 391-15-15).

Pile-up rejection

A technique used to identify and reject pulses (signals) which are piled up.

p-i-n detector

A detector consisting of an intrinsic or nearly intrinsic region between a p and n region.

Pole-zero cancellation

A pulse-shaping method, usually by means of a differentiator, eliminating undershoots of long duration (IEC Publication 340).

Pulse decay time (t_d)

The interval between the instants at which the instantaneous value last reaches specified upper and lower limits, namely, 90% and 10% of the peak pulse value unless otherwise stated. (In the case of a step function applied to an amplifier that has simple CR-RC shaping, the decay time is given by $t_d = 3.36$ CR.)

Pulse amplifier

An electronic amplifier designed to provide within the limits of its normal operating characteristics a single output pulse for each input pulse (IEV 391-11-02).

Pulse rise time (t_r)

The interval between the instants at which the instantaneous value first reaches specified lower and upper limits, namely, 10% and 90% of the peak pulse value unless otherwise specified. (In the case of a step function applied to an RC low-pass filter, the rise time is given by $t_r = 2.2$ RC. In the case of a step function applied to an amplifier that has simple CR-RC shaping, i.e., one high-pass and one low-pass RC filter of equal time constants, the rise time is given by $t_r = 0.57$ RC.)

Resolution, energy (per cent) (see *Energy resolution (per cent)*)

Semiconductor detector

An ionizing detector using a semiconductor medium in which an electric field is provided for the collection at the electrodes of the excess charge carriers produced by ionizing radiation (IEV 391-08-13).

Space-charge generation (in a semiconductor radiation detector)

The thermal generation of free charge carriers in the space-charge region.

Space-charge region (of a semiconductor radiation detector)

A region in which the net charge density is significantly different from zero (see also *Depletion region*).

Spectral line

A sharply peaked portion of the spectrum that represents a specific feature of the incident radiation, usually the full energy of a monoenergetic radiation.

Spectrum (radiation)

A distribution of the intensity of radiation as a function of energy or its equivalent electric analog (such as charge or voltage) at the output of a radiation detector.

Standard source diameter

The diameter of the X-ray emission source which is used to measure the response characteristics of the spectrometer. Unless otherwise specified, this is assumed to be a point source.

Standard working axis (of a semiconductor X-ray energy spectrometer)

A straight line drawn between the centre of the entrance window on the detector and the specified location of the source of X-rays.

Surface barrier contact

A rectifying contact that is characterized by a potential barrier associated with an inversion or accumulation layer; said inversion or accumulation layer being caused by surface charge resulting from the presence of surface states and/or work function differences.

Surface barrier semiconductor detector

A semiconductor detector in which the potential barrier due to the junction results from a superficial inversion layer (IEV 391-09-42).

Sweep-out time, charge (of a semiconductor radiation detector) (see *Charge collection time*)

Tail or tailing (on a monoenergetic peak)

Any peak shape distortion which does not comply with the limits defining the full energy peak intensity and which does not come from a source of radiation other than the monoenergetic source in question.

Total depletion voltage (of a semiconductor detector)

The reverse voltage at which the depletion layer extends over essentially the whole thickness of the semiconductor.

Total detector dead layer (of a semiconductor detector)

All insensitive materials of the detector system which the radiation must penetrate to reach the sensitive volume (IEC Publication 596).

Totally depleted detector

A detector in which the thickness of the depletion region is essentially equal to the thickness of the semiconductor material.

Transmission semiconductor detector

A semiconductor detector whose thickness, including its entrance and exit windows, is sufficiently small to permit the radiation to pass completely through the detector (IEV 391-09-47).

Window (of a semiconductor radiation detector) (see *Dead layer thickness*)

Window amplifier (see *Biased amplifier*)

Working distance

The distance, measured along the working axis, between the source of X-rays and the outermost window on the detector.

4. Symbols

A = intensity of full energy monoenergetic peak; total number of counts in a full energy peak

A_b = number of counts in the background under a peak

A_E = intensity of spectral peak at energy E; the total number of counts in the full energy peak of energy E

A_{Mn} = intensity of backscattered Mn K_α peak

A_t = total peak area, number of counts in the full energy peak, plus background

a, b = constants characterizing noise

B = bandwidth

C = electrical capacitance

C_d = detector capacitance

C_c = calibrated capacitor used to couple a pulse generator to a circuit under test

C_{eff} = effective input capacitance of a preamplifier

C_f = feedback capacitance in the integrating loop of a charge-sensitive preamplifier

C_t = total capacitance at a preamplifier input

C_1 = the average number of counts per channel in five contiguous channels centred around the energy of 5.4 keV in the tail of a Mn K_α X-ray energy spectrum

C_2 = same as C_1 except 4.5 keV

C_3 = same as C_1 except 1 keV

Δ = FWHM of a monoenergetic spectral peak

Δ_E^A = FWHM, expressed in units of energy, due to amplifier noise

Δ_N^A = FWHM, expressed in channels, due to amplifier noise

Δ_Q^A = FWHM, expressed in units of charge, due to amplifier noise

Δ_E^D = FWHM, expressed in units of energy, due to detector noise

Δ_N^D = FWHM, expressed in channels, due to detector noise

Δ_Q^D = FWHM, expressed in units of charge, due to detector noise

ΔE_{max} = the maximum deviation, in units of energy, between the measured linearity curve and the ideal linear response curve

ΔN = a shift, expressed in channels, of the peak centre (modal) channel

Δ_E^O = FWHM, expressed in units of energy, due to all factors other than electrical noise

Δ_N^O = FWHM, expressed in channels, due to all factors other than electrical noise

Δ_E^S = FWHM for monoenergetic incident radiation, expressed in units of energy, including all spectral broadening effects

Δ_N^S = FWHM for monoenergetic incident radiation, expressed in channels, including all spectral broadening effects

Δ_E^T = FWHM, expressed in units of energy, due to the combined effect of detector and amplifier noise

Δ_N^T = FWHM, expressed in channels, due to the combined effect of detector and amplifier noise

Δ_Q^T = FWHM, expressed in units of charge, due to the combined effect of detector and amplifier noise

E = energy of a particle or photon

ε = average energy required to form one hole-electron pair in a semiconductor

e = electron charge

E_F = the energy corresponding to the maximum linear output of a spectrometer

e_{ni} = equivalent root-mean-square noise voltage referred to the preamplifier input

e_{no} = root-mean-square noise voltage

e_{qi} = root-mean-square noise in units of charge at the amplifier input

F = Fano factor, the ratio of the dispersion (square of the standard deviation) of real (or actual, true, empirical) statistics of charge carriers to the dispersion of calculated Poisson statistics

G_B = gain of a biased amplifier (dimensionless)

φ = noise spectral power density

i = detector noise current

I = electric current

I_d = detector leakage current

I_o = diode equivalent Gaussian noise current in a specified frequency band

INL = integral non-linearity; the maximum deviation from linearity expressed as a percentage of the maximum linear output

k = Boltzmann's constant

K = constant relating FWHM in units of energy to FWHM in units of charge

L_D = differential non-linearity of an amplifier

L_i = integral non-linearity of a biased amplifier

L_I = integral non-linearity of an amplifier

N = channel number corresponding to the maximum of a monoenergetic spectral peak

N_{avg} = average number of counts in all channels of a multichannel pulse-height analyzer spectrum

N_B = equivalent number of channels suppressed by a biased amplifier

N_p = the total number of counts in the modal (peak centre) channel of the Mn full energy peak from a Mn K_α X-ray energy spectrum

N_x = number of counts in channel X of a multichannel pulse-height analyzer spectrum

P_1 = the peak-to-tail ratio at 5.4 keV for a Mn K_α X-ray energy spectrum

P_2 = the peak-to-tail ratio at 4.5 keV for a Mn K_α X-ray energy spectrum

P_3 = the peak-to-tail ratio at 1 keV for a Mn K_α X-ray energy spectrum

Q = electric charge

R = electrical resistance

R_c = resistor used in parallel with C_c to effect pole-zero cancellation

R_f = a resistor in parallel with C_f (used to stabilize the operating point of the first active element in a preamplifier)

r_i = input data rate to a system or device

R_L = detector load resistor

r_o = output data rate of a system or device

S_L = output pulse-height stability

S_M = sensitivity of MCA or ADC/computer system expressed in energy units of eV/channel

T = absolute temperature

t_c = charge collection time in a detector

t_d = dead time in a device or system

t_e = observed detector rise time due to the combined effects of the charge collection time and detector electrical rise time

t_p = detector electrical rise time

t_r = rise time (10% to 90%)

τ = time constant

τ_c = time constant of a CR network used to simulate the rise of a pulse from a radiation detector

τ_d = decay time constant

t_w = width of a pulse, in time units, at the baseline established by the discriminator threshold level

V = electric voltage

V_a = amplitude of amplifier output voltage

V_d = detector bias voltage

V_D = depletion voltage

V_p = amplitude of the voltage step impressed on C_c by the pulse generator

W_E = window attenuation index at energy E as determined by the spectrum from a standard target excited with ^{55}Fe

X = channel number in a multichannel analyzer (MCA) or computer display of a photon energy spectrum

Z = atomic number

Z_0 = characteristic impedance

λ = the characteristic wavelength associated with an X-ray photon

δ_E^S = FWTM for monoenergetic incident radiation, expressed in units of energy, including all spectral broadening effects

δ_N^S = FWTM for monoenergetic incident radiation, expressed in channels, including all spectral broadening effects

δ_E^T = FWTM, expressed in units of energy, due to the combined effect of detector and amplifier noise

δ_E^O = FWTM, expressed in units of energy, due to all factors other than electrical noise

δ_N^T = FWTM, expressed in channels, due to the combined effects of detector and amplifier noise

5. Introduction

5.1 *Detector system*

A semiconductor detector is analogous to a gas ion chamber in which the gas has been replaced by a solid. Figure 1, page 41 illustrates this type of detector and its preamplifier configuration. The detector consists of a semiconducting crystal between two conducting electrodes. A potential difference is established between the electrodes thereby producing an electric field in the semiconductor. When an X-ray photon enters the semiconductor it produces free charge carriers in the crystal, the number of which is proportional to the energy lost by the X-ray photon. The charge motion resulting from the influence of the electric field produces an induced current pulse in the external circuit. This current represents the basic signal information and the integrated current pulse is proportional to the energy lost by the X-ray. The pulses are routed to a multichannel pulse-height analyzer (MCA) where they are sorted and stored according to the amplitude distribution to produce a pulse-height spectrum that corresponds to the X-ray energy spectrum. The MCA may be a dedicated instrument or an analog-to-digital converter (ADC) interfaced to a computer.

The semiconductor materials which are most frequently used for X-ray spectrometers (i.e., silicon and germanium) do not have sufficiently high resistivity to withstand large electric fields without excessive leakage currents. It is therefore necessary to use special techniques to limit the current flow through the semiconductor device. This is usually accomplished by utilizing the space charge region of a reverse biased diode junction as the detector sensitive volume. Silicon and germanium are the only semiconductor materials which are presently available with sufficient crystalline perfection and purity to be generally useful for this type of device, although work is progressing on other semiconductors such as HgI_2, CdTe and GaAs.

Although both Si and Ge crystals are available in very pure form, the electrically active impurity level is sometimes too high to allow fabrication of usefully large detectors. This limitation can be overcome by using mobile lithium ions to compensate the electrically active impurities. If the lithium compensation technique is used, the germanium semiconductor device is subject to inherent stability problems since the compensation can be classed as highly unstable at room temperature and therefore lithium-compensated germanium devices must be stored at reduced temperatures. In silicon the compensation is quasi-stable, with the degree of stability depending on the presence of other impurities in the crystal and on the details of the device fabrication.

Since there is no internal gain in the type of semiconductor detector considered here, the problem of noise in the detector and in the preamplifier circuits is significant, particularly at low X-ray energies. Consequently, both the semiconductor detector and first stage of the preamplifier are usually operated at low temperature to reduce the thermal noise.

Energy resolution is one of the most important characteristics of an X-ray energy spectrometer since it sets the limit on the ability to resolve closely spaced lines. Figure 2, page 42 shows the K_α separation of adjacent elements as a function of atomic number.

In comparing instruments it is necessary also to examine the other specifications, since improved energy resolution may be provided at the expense of other important parameters such as count-rate capability, gain stability, and detector size (efficiency).

The limit resulting from the statistical uncertainty involved in the process whereby the incident X-ray energy produces free charge carriers is a fundamental limit on energy resolution and is discussed in detail in Sub-clause 5.2.

Preamplifier and detector noise also affect the resolution and are examined in Sub-clauses 5.3 and 5.4. Charge loss from trapping and recombination can also have significant effects on the spectral quality. The peak-width broadening from charge loss typically increases with increasing energy since the fluctuation in the amount of charge trapped usually increases with total charge. "Partially dead" regions or layers can also produce spectral distortion in the form of low energy tails, non-linearities, and loss of detector efficiency at low energies. These effects are described in Sub-clause 5.5.

Electronic stability is an important variable which includes not only the stability of the preamplifier, but also that of other parts of the system, such as the main amplifier and the MCA.

Effects of high count-rate such as pulse pile-up and d.c. level shifts are also important. Every time an event produces a pulse in the amplifying equipment, the d.c. levels throughout the system are perturbed and take some time to return to their original values. If another event occurs within this time interval, its effective output pulse height may be altered, thereby contributing to spectral distortion.

5.2 *Statistical limit of resolution*

If Poisson (random) statistics are applied to the process of the X-ray energy loss mechanism by free charge carrier formation, then it would be possible to calculate the statistical broadening of a monoenergetic X-ray peak from FWHM $= 2.35\sqrt{\varepsilon E}$, where E is the energy of the incident radiation and ε is the average energy required to create a free electron-hole pair. Frequently used values of ε at 77 K are 3.8 eV/pair for silicon and 3.0 eV/pair for germanium. In fact, the charge production process does not follow Poisson statistics because the multiple events that occur in the energy loss process are correlated. Therefore, the statistical formula is usually modified by inserting a correction factor F (called the Fano factor), resulting in the expression FWHM $= 2.35\sqrt{\varepsilon F E}$. This corrects for the fact that the observed broadening is substantially less than that predicted by Poisson statistics. For Si and Ge, F is not accurately known, but measurements have indicated limits between 0.05 and 0.15.

Since it is not possible to measure the Fano factor and the resolution broadening caused by charge carrier trapping independently, the two effects are frequently combined in the value assumed for F. This is equivalent to the assumption that the charge loss (trapping) is a constant fraction of the free charge created.

5.3 *Preamplifier noise*

Preamplifier noise arises from a number of sources. One is the thermal noise in the input field effect transistor (FET) of the preamplifier (see Figure 1, page 41). This is usually minimized by cooling the FET and using selected FETs. With regard to the FET contribution, the signal-to-noise ratio (S/n) decreases with increasing total capacitance at the FET gate and therefore decreases with increasing detector area. Thus, there is an important compromise between detector size and the observed S/n. Parasitic capacitance also affects S/n. Consequently, the physical configuration of the detector and preamplifier package is critical. The resistors R_f and R_L shown in the circuit of Figure 1a, page 41, also can be important sources of noise. In order to minimize the effect of stray capacitance and resistor noise, C_c and R_L are usually eliminated by d.c. coupling the detector to the gate of the first FET as in Figure 1b, page 41. Hence all of the current caused by the radiation must flow through R_f or the high impedance gate of the field effect transistor. This can change the FET operating point and the overall gain of the system, unless there is sufficient d. c. feedback via R_f to provide the required count-rate versus gain stability. The greater the feedback resistance (R_f) the smaller the resistor noise contribution but the poorer the count-rate energy product capability. This presents an important compromise consideration between noise broadening of the resolution and performance at high count-rates.

In this respect, it should be pointed out that it is not enough to specify just the simple count-rate capability because it is the product of count-rate and average radiation energy which is important, for example 100 keV X-rays present 20 times the count-rate problem of 5 keV X-rays. Other more sophisticated feedback mechanisms such as optical feedback, d.c. feedback, or pulsed optical feedback can be used in place of R_f and are in common usage as methods for reducing noise. However, these techniques also involve similar resolution versus count-rate compromises.

Figure 3, page 43 shows the combined effects of preamplifier noise and statistics for two values of Fano factor, amplifier noise and ε. The preamplifier contribution is independent of energy, while the statistical broadening varies as the square root of the energy. At a noise level of about 400 eV, the preamplifier noise dominates over the entire range of interest for the *K*-lines of the stable elements, while with 100 eV noise, the noise and statistical effects are about equal at the photon energy of 3.7 keV.

5.4 *Detector noise*

Leakage current in the detector element and Johnson noise in the detector series resistance can also contribute to system noise and resolution broadening. In integrated X-ray spectrometer systems, it is usually not possible to distinguish unambiguously between series noise sources (e.g., the FET series noise) and parallel noise sources such as detector leakage current, feedback resistor, and microphonics. Since the parallel noise predominates at lower frequencies, some indication of the presence of detector current noise or excess feedback noise can be obtained by examining the noise as a function of amplifier passband.

5.5 *Charge loss*

Loss of free charge carriers because of trapping in the semiconductor crystal can be a significant source of spectral distortion. The peak width broadening from this effect is proportional to the energy of the X-ray and therefore more pronounced at higher energies. Charge trapping, which is a function of detector bias voltage, frequently results in low energy tails on monoenergetic spectral lines. The effect is therefore often more readily apparent in the full width at tenth maximum of the peak height (FWTM) than in the FWHM of the spectral peak. The peak-to-valley ratios of $K_\alpha - K_\beta$ X-ray lines are also quite sensitive to this effect. The FWTM performance of the system is more important than it might appear on superficial examination. For example, if it is desired to determine a 10% X-ray fluorescence contribution from one element in the presence of a 90% contribution from the next higher element, the FWTM is more relevant than the FWHM.

Windows and dead layers, even when not an intimate part of the detector element, contribute to loss of efficiency at low X-ray energies. In addition, charge loss in "partially-dead" layers in the portion of the detector adjacent to the entrance window can result in both a loss of full energy peak efficiency and in undesirable spectral distortion in the form of a low energy tail, spurious peaks, and non-linearity.

Since major charge loss problems frequently occur around the outer periphery of the detector active area, these problems tend to be very sensitive to the source-detector geometry employed in the measurement. Consequently, for specification parameters where charge loss is a key variable, it is essential to define the source-detector geometry. This geometry can be conveniently defined in terms of the standard working axis, standard working distance, and standard source diameter. For detectors used in microanalysis applications, the standard source diameter is negligible (a point source).

For the measurements described herein, it is desirable to make a distinction between background and non-ideal peak shapes such as asymmetries, tails, spurious peaks, etc. As used herein, the term background will refer only to non-ideal spectral response which results from radiation that is not a part of the monoenergetic X-ray line of interest.

5.6 *Electronic stability and extraneous noise*

The gain stability of the system and excess noise from spurious electrical effects or from microphonics can affect the performance of the system. The FWTM is frequently more sensitive to these problems than the FWHM.

5.7 *Count-rate effect.*

5.7.1 *Pulse-shape considerations and distortion by pulse pile-up*

In order to optimize the signal-to-noise ratio as well as to provide reasonable count-rate capability, it is necessary to restrict both the upper and lower limits of the amplifier passband. At any given count-rate, the width (in time) of the resulting pulse will determine the probability that the preceding or succeeding pulse will be distorted by pulse-on-pulse or pulse-on-tail pile-up. Choice of the type of pulse shaping and the time constants associated with the pulse therefore involves an important compromise between optimum energy resolution at low count-rates and the performance of the system at high count-rates. Preamplifier noise can frequently be minimized by using relatively long pulse shaping time constants ($\simeq 10\ \mu s$). However, the resulting optimum shaping time constant for minimum noise can be inconsistent with the count-rate requirements of the user. Consequently, energy resolution specifications should always be accompanied by either the maximum applicable count-rate and detailed information on the pulse shape, or a detailed description of the change in FWHM and FWTM as a function of count-rate at a specified energy. The latter description of performance is particularly useful in cases where the instrument is to be used in quantitative analysis where changes in resolution with changing count-rate would seriously complicate analysis of the resulting data.

The usual shaping time constant number associated with the amplifier is by itself only marginally useful in predicting count-rate capability. The pile-up limitation of the system is primarily determined by the width of the pulse near the baseline.

For a given nominal time constant, this time interval can vary by a factor of two or more, depending on the type of pulse shaping and the convention used for assigning a time constant value. Although the attainment of low pile-up requires that the characteristic width of the pulse be small compared to the mean interval between pulses, it is also necessary that the pulse return closely to the baseline (average d.c. level) in a time interval small compared to the mean interval between pulses. Many preamplifier-amplifier systems utilize a design principle referred to as pole-zero (PZ) cancellation to minimize undesirable undershoots.

Failure to achieve accurate PZ cancellation can degrade the FWHM and FWTM and can also result in low or high energy tails on spectral peaks, depending on whether an undershoot or overshoot exists. This source of distortion is particularly important at high count-rates.

5.7.2 *Baseline (d.c. level) shifts, baseline (d.c.) restoration, count-rate induced gain shifts and non-linearities*

A count-rate induced d.c. level shift anywhere within the electronic amplifying chain will introduce gain shifts and non-linearities whenever the d.c. level exceeds the linear dynamic range of that portion of the signal processing chain. Also, when the limit of the linear dynamic range is approached, statistically induced fluctuations in the d.c. level can exceed this limit, resulting in peak broadening and other related spectral distortions. In addition, a short-term d.c. level shift at the output of the amplifier system will produce an equivalent shift in the magnitude of the output voltage pulse presented to the ADC of the MCA or single-channel analyzer, thereby degrading the resolution. Customarily, these problems are reduced by using d.c. feedback and by using a baseline restorer (BLR) at the output of the amplifying chain. Baseline restoration can also add a noise contribution which depends on the restoration mode and restoration rate (time constant).

Consequently, when specifying resolution, stability, gain shift, linearity, etc., as a function of count-rate, it is essential that the following information be stated:

a) the energy for which the performance is specified;

b) details of the pulse shaping;

c) details of restoration mode;

d) details of pile-up rejection.

Specifications as a function of count-rate shall be obtained at the same operating conditions (e.g., same pulse shape, feedback configuration, restoration mode, etc.). This requirement is particularly relevant to applications where it is not practical to reoptimize the spectrometer system every time the product of the count-rate and the energy changes.

5.7.3 *Overload recovery*

Overload pulses produced by high-energy radiation events which exceed the dynamic range of the amplifying equipment can produce undesirable effects such as baseline overshoot or undershoot and system paralysis (dead time). However, since good overload performance may compromise other system characteristics it should not be emphasized in those applications where overload signals are not a significant problem.

5.8 *Detector material selection: germanium versus silicon*

The two semiconductor detector materials which are presently available for high-resolution X-ray energy spectrometers are germanium and silicon. The relative potential advantages and disadvantages of each are summarized as follows:

Germanium

Advantages

1) Higher atomic number (Z) which results in better efficiency at high energies.

2) The smaller value of ε reduces the relative importance of noise (see Sub-clause 5.3) and possibly the statistical contribution to the resolution (see Sub-clause 5.2).

Disadvantages

1) Higher efficiency at high energy produces more background problems from high-energy sources.
2) An equal linear thickness for the dead layer (entrance window) corresponds to a much greater efficiency loss at low energy.
3) Worse low-energy tailing on low-energy peaks.
4) High efficiency at high energy increases the probability of amplifier overload.

5) High Z results in increased spectral complication by escape peak problems and a more complex relation between efficiency and energy.
6) Smaller band-gap increases the potential detector leakage current noise problems.

Silicon

Advantages

1) Dead layer effects are smaller.
2) It exhibits relative freedom from escape peak complications in complex spectra.

3) Silicon is less sensitive to high-energy background problems.
4) Silicon can be used at higher temperatures with less detector noise contribution.

Disadvantages

1) Efficiency is lower at high energy (>30 keV).
2) Higher average energies required to form an electron-hole pair (i.e., larger ε).

5.9 *Detector efficiency*

The full-energy peak efficiency of a semiconductor X-ray energy spectrometer is energy dependent. It is a function of the physical size and shape of the detector, the presence of windows or dead layers on the detector and its container, charge trapping problems within the detector, the Z of the detector material, and the energy of the K_{abs} edge of the semiconductor.

Typical graphs of efficiency versus energy are illustrated in Figure 4, page 44 The low-energy response threshold is established by absorption in the window of the detector entrance surface. In addition, any partially-dead layer within the detector near its entrance window may contribute to the drop in efficiency at low energy and may also result in low-energy background counts for peaks at lower energies (i.e., a low-energy tail on a monoenergetic X-ray peak). Variations of full-energy peak efficiency as a function of energy are also caused by the sharp change in the absorption coefficient near the K_{abs} edge. Since this sudden increase in cross-section results in a high probability of interaction near the entrance window on the semiconductor, dead or partially-dead layers adjacent to the entrance window can cause large drops in the full-energy peak efficiency at energies just above the K_{abs} edge.

The drop in efficiency at high energy depends on the sensitive depth and volume of the detector. The efficiency at high energies, as well as the spectral quality (low-energy tailing) can also be affected by the existence of a partially-dead layer near the back contact to the sensitive region, poor charge collection throughout the sensitive region, or by isolated partially-dead layers within the sensitive volume.

5.10 *Resolution of adjacent lines and line-to-background ratio*

The question of when two adjacent spectral lines are "resolved" is somewhat subjective since it depends on the particular experimental conditions and performance criteria. For example, when attempting to analyze a line in the presence of a nearby much stronger line, it may be the FWTM of the more intense line that determines whether the lines are "resolved". When attempting to analyze a line in the presence of a much more intense higher-energy neighbour, it may be the low-energy tailing from the more intense line that establishes the sensitivity and accuracy of the measurement. This standard does not attempt to establish an arbitrary – and possibly misleading – definition to determine if two adjacent lines are resolved. Rather, the approach adopted in this standard is that of defining key characteristics of the spectral response so that the user can interpret the instrument specification with respect to his own needs.

The concept of line-to-background ratio has traditionally been of considerable usefulness to the X-ray analyst. However, the line-to-background ratio in any particular application depends not only on the performance of the X-ray energy analyzer, but also on other factors such as the method of X-ray excitation (e.g. electron, heavy ion, secondary X-ray, radioactive source), the character of the fluorescing sample, and geometrical arrangement of the exciting source, target, and detector. Since these latter factors are frequently beyond the control of the X-ray energy spectrometer manufacturer, this standard does not include test procedures for line-to-background ratio determination.

However, standards for specifying the characteristic spectrometer parameters such as FWHM, FWTM, peak-to-tail, and peak-to-valley ratios which directly affect the line-to-background ratio have been included (e.g. if the FWHM doubles, the line-to-background ratio will decrease to one-half, all other factors remaining constant)

5.11 *Miscellaneous other effects*

5.11.1 *Microphonics*

Microphonic noise generation may be a serious source of resolution broadening. In cryogenic systems, mechanical vibrations of the input circuit components relative to surfaces at different potentials can introduce noise. Such vibrations can be produced by bubbling of liquid nitrogen, turbulence from automatic nitrogen transfer systems, vibration of other equipment in contact with the detector cryostat, and environmental noise. A change of capacitance between the FET gate and the high voltage (detector bias 1 000 V) of only 5×10^{-7} pF is sufficient to generate a microphonic signal equivalent to that of a 10 keV X-ray. Since the typical stray capacitances are of the order of 1 pF, mechanical motions (within the frequency pass-band of the shaping amplifier) of approximately one part in 10^7 are significant. Since most of the vibration problems are at relatively low frequency, much of the microphonic noise is filtered out by the low-frequency response of the amplifier. Consequently, microphonic problems become more serious at long shaping time constants. This problem involves the excitation of internal mechanical resonances by internal or external vibrations and is quite complex. Microphonics problems can be studied in a qualitative way by exciting the system with an audio speaker driven by a variable frequency generator. However, because of the wide diversity of detector mechanical configurations available, it would be difficult to establish a standard for microphonics. None the less, the user should be aware of this potential problem.

5.11.2 *Secondary fluorescence*

Secondary fluorescence of metal parts of the cryostat, detector, and preamp mount and the metal electrodes on the detector can cause spectral distortion in the form of spurious peaks in the spectrum. Detector producers are urged to give detailed information about the material, especially of related components, the detector mount itself and the contact zone. Additionally, the geometry of the preamp FET relative to the radiation main axis is needed to assess the influence of the secondary fluorescence.

5.11.3 *Liquid nitrogen loss rate*

Most semiconductor X-ray analyzers use liquid nitrogen for cooling the detector and preamplifier. The efficiency of the cryostat design is directly reflected in the liquid nitrogen consumption rate. Excessive liquid nitrogen consumption aggravates microphonics, and increases the operating cost, inconvenience, and the chance of accidental warm-up. This performance parameter is usually covered by specifying the capacity of the liquid nitrogen reservoir and the minimum guaranteed holding time (of the temperature).

6. General

6.1 *Definition of semiconductor X-ray energy spectrometer*

A semiconductor X-ray energy spectrometer is an instrument which utilizes the proportionality between the energy of an X-ray and the number of free electron-hole pairs created in a semiconductor radiation detector by that X-ray as a means of measuring the energy of the X-ray. In this standard the spectrometer is assumed to consist of the semiconductor detector, preamplifier, means for cooling, encapsulation, required vacuum and mechanical housings, amplifier, power supplies, and other required analog electronics. For the purposes of this standard, analog-to-digital data conversion and subsequent data-handling equipment are not considered to be a part of the spectrometer, even though it is recognized that they are an essential ingredient in establishing the total system performance. In addition, sample stages, the X-ray emitter, and means for exciting same (e.g., radioactive sources, electron beams, etc.) are considered to be ancillary equipment and not part of the spectrometer.

6.2 *General precautions and specifications*

The following general precautions and specifications are relevant to all of the test procedures described herein.

Maximum detector bias voltage, rate of bias voltage change, radiation flux ratings, line voltage, maximum detector temperature, and other manufacturer's specification limits should not be exceeded or permanent damage to the instrument may result.

The values of the parameters specified should be reproducible within the precision of the measurements after the performance of any one or all of the tests performed. Care should be taken to ensure that power-line noise, earth loops, mechanical vibration, and the characteristics of ancillary test equipment do not substantially influence the test results.

Relevant test conditions such as pulse shaping (type and time constants), detector bias, etc., shall be clearly stated. In no case shall performance data which require change in operating condition or mode be presented as a plotted envelope or table (e.g., if energy resolution versus count-rate is plotted, all data points must correspond to the same operating conditions). If it is desired to show results for several operating modes (e.g. time constants), then these should be shown as a family of curves with operating mode as a parameter.

Since the semiconductor X-ray energy spectrometer user seeks energy and intensity distribution information, it is reasonable to specify system performance in terms of energy spectrum distortion and variations in the system detection efficiency as a function of energy. Consequently, many of the performance parameters contained herein are described in terms of deviations from ideal behaviour.

In order to establish standardized test procedures which are independent of the various sources of X-rays which might eventually be used with the instrument, readily available radioactive sources have been specified for the test procedures. Whenever possible, isotopes having simple energy spectra have been selected. This is particularly important in resolution versus count-rate tests where multiple lines greatly complicate the interpretation of the data. An attempt has been made to specify standard sources covering the energy range of interest for both Si and Ge detectors when used with characteristic elemental X-rays. It is recognized that special applications or requirements may necessitate the use of additional X-ray energies to adequately characterize the instrument.

6.3 *Simulating the signal pulse of a detector*

A pulse from a pulse generator is useful for measuring the electronic noise contribution to the resolution, electronic linearity, gain stability, and also for energy calibrations. In order for all sources of noise, drift, etc., to be sampled by the test pulse, the charge shall be injected into the input of the preamplifier as illustrated in Figure 5, page 45 The type of pulse generator shown in Figure 6, page 46, is frequently referred to as a tail pulse generator. Pulse generators which produce a square pulse are also occasionally used instead of tail pulse generators.

Test pulses applied by capacitive coupling cannot precisely simulate true signal pulses. The exponential decay τ_d shown in Figure 6 corresponds to an uncancelled pole which results in an undershoot at the amplifier output. Pole-zero cancellation of the charge coupling capacitance is not appropriate to this problem, since it would result in excess noise at the preamplifier input. For a square pulse, droop in the pulse corresponds to a long time constant pole and, in addition, the negative going portions of the pulse will produce a pulse of the wrong polarity in the amplifier and possibly result in undesirable baseline shifts.

Consequently, pulse generators should not be used to generate the high and variable count-rate required for count-rate effect measurements. In addition, it is preferable to turn the pulser off during X-ray resolution measurements, particularly if the measurements are performed at high count-rates and/or with long pulse shaping time constants. Some systems, for example amplifiers with gated BLR, may not tolerate the undershoot from a tail pulse generator or the opposite polarity signal produced by a square pulse generator

7. **Energy resolution and spectral distortion**

7.1 *Noise measurement by pulse-height distribution (preferred method)*

The electronic and detector noise contribution to the resolution width can be determined by this method only if the instrument is provided with a pulser coupling capacitor (C_c) as shown in Figure 5. The spectrometer is connected to a multichannel analyzer as shown in Figure 5. With all elements of the system operating within their linear range and with the detector at its specified operating voltage, expose the detector to an appropriate X-ray source (e.g., 5.9 keV Mn K_α from ^{55}Fe) and accumulate a spectrum. The system gain and pulse amplitude shall be such that the FWHM of the X-ray peak is at least eight channels and that of the pulser peak is at least five channels. (For MCAs with a small number of channels it may be necessary to use a biased amplifier or a digital off-set in the ADC following the main amplifier to achieve this condition.) Remove the X-ray source and calibrate the pulse generator by setting its output amplitude dial to the appropriate X-ray energy (e.g. 5.9 keV) and adjusting the calibration controls until the pulser peak and the X-ray peak have the same peak centre (modal) channel. With the source removed, and with the system gain such that the

FWHM of the pulser peaks is at least five channels, accumulate the two peaks corresponding to pulse generator equivalent output energies E_1 and E_2 in channels X_1 and X_2 as shown in Figure 7, page 47. The system total noise line width is defined as:

$$\Delta_E^T = \left(\frac{E_1 - E_2}{X_1 - X_2}\right) \Delta_N^T \qquad (1)$$

where Δ_N^T is the interpolated number of channels corresponding to the full width of the peak at one-half the maximum height of the peak.

The FWTM is defined as:

$$\delta_E^T = \left(\frac{E_1 - E_2}{X_1 - X_2}\right) \delta_N^T \qquad (2)$$

where δ_N^T is the number of channels corresponding to the full width of the peak at one-tenth the maximum height of the peak.

If the pulse generator is triggered by line frequency, this technique may not detect the presence of noise which is correlated with line frequency. This problem may be avoided by using a pulse generator with an internal trigger which is asynchronous with line frequency.

When stating the total noise line width, complete information on the pulse shaping (including the full-pulse width) shall be given (e.g. 2 µs CR-RC, or semi-Gaussian with four 2 µs CR integrations and one 2 µs RC differentiation). If baseline restoration (BLR) and/or gating techniques are used, the characteristics of the BLR and/or gating shall also be stated (see Clause 5).

7.2 *Alternate techniques for noise measurement*

7.2.1 *Noise measurement by oscilloscope and r.m.s. voltmeter*

An alternative method of measuring noise employs the system shown in Figure 8, page 88. The root-mean-square (r.m.s.) noise voltage level is indicated on an r.m.s. voltmeter having a flat-band frequency response extending to at least ten times the band centre frequency of the amplifier pulse-shaping networks. In addition, the amplifier incremental-gain shall be constant down to below the noise level (a biased amplifier, BLR, or gating can render this measuring technique useless). The same constraints regarding operating conditions and reference specifications outlined in Sub-clause 7.1 apply here also. The pulse generator is calibrated as in Sub-clause 7.1 except that the oscilloscope is used to compare the pulse heights of the source and pulser. A pulse generator-pulse equivalent to energy E_p is applied and the resulting amplifier output V_a is measured in the oscilloscope. The pulse generator is switched off and the r.m.s. noise voltage e_{no} is read from the voltmeter. The system FWHM noise linewidth is given by:

$$\Delta_E^T = 2.35 \cdot a \cdot e_{no} \left(\frac{E_p}{V_a}\right) \qquad (3)$$

where a is 1.11 for a sine-wave-calibrated average-reading voltmeter and unity for a true r.m.s. voltmeter. The value of E_p/V_a can also be obtained by using a monoenergetic X-ray source of energy E_p.

7.2.2 *Noise approximation from X-ray spectral resolution*

The electronic noise contribution to the resolution broadening can also be approximated from the variation of X-ray peak width as a function of energy as given by:

$$\Delta_E^{T} = \left(\frac{(\Delta_{E_1}^{S})^2 \cdot E_2 - (\Delta_{E_2}^{S})^2 \cdot E_1}{E_2 - E_1}\right)^{1/2} \tag{4}$$

where Δ_E^T is the FWHM noise linewidth of equation (3) and $(\Delta_{E_1}^S)$ and $(\Delta_{E_2}^S)$ are the FWHM total linewidths for the peak at energies E_1 and E_2, respectively (see also Sub-clause 7.4).

Considerable caution needs to be applied in the use of equation (4), since it is prone to error for the following reasons:

a) the value for Δ_E^T may be the result of taking a small difference between large numbers and therefore, the error propagation problem is significant;

b) equation (4) assumes that the fractional charge loss effects are independent of energy, an assumption that is questionable below 3 keV or over a large energy range;

c) the X-ray peaks are multiplets (e.g. $K_{\alpha 1}$, $K_{\alpha 2}$). The separation of these multiplets is a function of energy and whether the peak is a K or L or M line. This source of variable peak broadening has not been taken into account in equation (4).

7.3 *Noise linewidth as a function of amplifier time constants*

Information concerning the series and parallel noise contributions can be obtained by plotting noise linewidth as a function of amplifier time constants. In addition, such a plot can give important information regarding the count-rate versus energy resolution compromise. To perform this measurement, the method of Sub-clause 7.1 or 7.2 is employed with an amplifier having adjustable shaping time constants. The results are displayed as a plot of noise linewidth as a function of pulse-shaping time constants (with other possible variables such as BLR as a parameter).

7.4 *X-ray linewidth measurements by pulse-height distribution*

7.4.1 *X-ray sources*

The following radioactive sources are recommended for specification of energy resolution:

a) ^{55}Fe 5.9 keV – Mn K_α ($K_{\alpha 1}$ – 5.898, $K_{\alpha 2}$ – 5.887);
b) ^{109}Cd 22.162 ($K_{\alpha 1}$) and 21.988 ($K_{\alpha 2}$) keV Ag K X-rays and 88 keV gamma-ray;
c) ^{57}Co 6.4 Fe K_α ($K_{\alpha 1}$ – 6.403, $K_{\alpha 2}$ – 6.390) and 14.4, 122, and 136 keV gamma-rays (not recommended for count-rate effect measurements).

If resolution is specified at one energy only, ^{55}Fe is the preferred source. The 5.9 keV Mn X-ray represents a reasonable compromise between amplifier noise broadening and other detector resolution broadening effects. The lines above 30 keV are relevant mostly to Ge detectors. To prevent spectral distortion from backscattered radiation, the source backing thickness and Z should be kept as small as possible

If lower-energy lines are desired, they may be obtained by secondary fluorescence of a target such as the standard glass described in Clause 12.

In case a secondary fluorescent target is used as a source of X-rays for resolution measurements, the background from the continuum should be subtracted before determining N_X (the counts in channel X). A suitable technique for background subtraction is described in Sub-clause 12.1 of this publication and Sub-clause 4.1 of IEC Publication 340.

7.4.2 *Spectral resolution*

These tests are carried out using the system of Figure 5, page 45 and one of the radiation sources listed in Sub-clause 7.4.1. The source is located on the standard working axis of the detector at the standard working distance. The active diameter of the source must not significantly exceed the standard working diameter. For those cases where the source is a true characteristic X-ray, the location of the centres of the K_α and K_β peaks can be used to obtain the calibration:

$$S = \left(\frac{E_1 - E_2}{X_1 - X_2}\right) \tag{5}$$

For other cases, or if the K_α and K_β are not sufficiently well resolved, the pulser technique of Sub-clause 7.1 may be used to obtain calibration. The results should be expressed as the FWHM and FWTM. The FWHM is obtained from the relation:

$$\Delta^S_E = \left(\frac{E_1 - E_2}{X_1 - X_2}\right) \Delta^S_N \tag{6}$$

where Δ^S_N is the full width (in interpolated fractional channels* of the peak at one-half its maximum amplitude. The FWTM is given by:

$$\delta^S_E = \left(\frac{E_1 - E_2}{X_1 - X_2}\right) \delta^S_N \tag{7}$$

where δ^S_N is the full width (in fractional channels) of peak at one-tenth its maximum amplitude. For a Gaussian peak: $\delta^S_N = 1.78\ (\Delta^S_N)$, thus $\delta^S_E = 1.78\ (\Delta^S_E)$.

The FWHM must be at least ten channels with a minimum of 40 000 counts in the peak centre (modal) channel. In reporting information on spectral resolution, the following shall be noted:

a) incident X-ray source and energy;

b) count-rate at which measurement was taken;

c) detector-source geometry (standard working distance and standard source diameter);

d) detailed description of detector and its collimator (shape, area, depth, Si or Ge, etc.);

e) detector operating bias;

f) system noise linewidth under the same operating conditions;

g) amplifier pulse-shaping parameters (including the full pulse width and BLR parameters).

---

* The method of interpolation shall be given by the manufacturer.

Another set of parameters of interest are those contributions to the detector linewidth caused by all factors other than electrical noise (e.g. statistical and charge collection problems). These quantities are found by subtracting the noise linewidth contributions in quadrature according to the relationships,

$$\Delta_E^{O} = \sqrt{(\Delta_E^{S})^2 - (\Delta_E^{T})^2} \quad (8) \qquad \text{and} \qquad \delta_E^{O} = \sqrt{(\delta_E^{S})^2 - (\delta_E^{T})^2} \quad (9)$$

It is relevant to point out that the resolution limit set by statistical considerations alone is given by:

$$\lim\,(\Delta_E^{O}) = 2.35\,\sqrt{F\,\varepsilon\,E} \qquad (10)$$

where:

Δ_E^{O} = FWHM linewidth in units of energy
E = X-ray energy
ε = average energy to form an electron-hole pair
F = Fano factor

The value of the Fano factor is not accurately established at the present time for either Si or Ge. Existing experimental data establish only a probable upper limit for F; however, $F = 0.1$ is commonly employed as a useful estimate of F.

7.5 *Peak-to-valley and peak-to-tail ratios*

Peak-to-valley ratios (Sub-clause 7.5.1) for two closely spaced peaks (e.g., the K_α and K_β of Mn from ^{55}Fe) and peak-to-tail ratios (Sub-clause 7.5.2) can be very sensitive indicators of spectral distortions caused by a variety of factors ranging from charge collection problems in the detector (or its partially-dead windows) to baseline instability and other related count-rate effects in the electronics. Peak-to-tail ratios can also be sensitive indicators of the detector system's line-to-background ratio capability.

When quoting peak-to-valley or peak-to-tail ratios complete details of the measurement conditions, including source-detector geometry (standard working distance and standard source diameter) amplifier time constant settings, input count-rate, and any other major variables which would significantly affect the measurement shall be clearly stated. The system parameter adjustments used for these specifications should be consistent with those used for specification of other performance parameters, such as FWHM, etc.

7.5.1 *Peak-to-valley ratio*

The peak-to-valley ratio between two specified peaks is defined as the ratio of the height of the larger peak to the height in the minimum of the valley between the two peaks.

Specifications of peak-to-valley ratios should be based on sufficient statistical information (i.e. number of counts per channel in the valley) to ensure a maximum statistical probable error of less than 5% in the peak-to-valley ratio.

7.5.2 *Peak-to-tail ratio*

This test consists of placing the active side of a standard ^{55}Fe source normal to and centred on the standard working axis and located at the standard working distance, adjusting gains so that at least ten channels appear across the FWHM, and counting until N_p counts (20 000 minimum) are accumulated in the peak centre channel (modal channel) at 5.9 keV. The number of counts in each of the groups of five contiguous channels centred around the energies of 5.4 keV, 4.5 keV and 1 keV, respectively, are averaged to give values C_1, C_2 and C_3 respectively.

The peak-to-tail ratios P_1, P_2 and P_3 are calculated from:

$$P_1 = N_p/C_1 \quad P_2 = N_p/C_2 \text{ and } P_3 = N_p/C_3 \qquad (11$$

Reduction of the peak-to-tail ratio may result from deterioration in system performance from contributions due to backscattering from the surroundings or source backing, high count-rates, system noise (ground loops, a.c. noise, etc.), improper equipment settings (misadjustment in pole-zero cancellation networks, non-optimum shaping times, etc.) or the presence of other radiation sources in the vicinity. Background from origins other than the ^{55}Fe source must be negligible in order to make this measurement meaningful.

This method for the determination of the peak-to-tail ratio can yield misleading results if there are other radionuclide impurities in the source which contribute to events in the tail. Errors resulting from impurities in the source can be detected by remeasuring the peak-to-tail ratio with an absorber placed between the ^{55}Fe source and the detector.

8. **Pulse-height linearity**

8.1 *System X-ray linearity by pulse-height analyzer method (preferred method)*

This technique measures the combined integral non-linearity of the detector system and the pulse-height analyzer. To determine the integral linearity of any component of the instrument chain, the effect of the other components must be measured and subtracted.

With the arrangement shown in Figure 5, page 45. the detector is exposed to a series of characteristic X-ray lines spanning the energy region of interest. Normally, a minimum of ten lines, more or less uniformly spaced over the region of interest is required for a good linearity check. These lines may be generated by secondary excitation induced with X-rays, gamma-rays, or charged particles. The lowest energy line should be less than 10% and the maximum-energy line greater than 90% of full-scale energy range of interest.

Care should be exercised to use only lines whose characteristic energy is accurately established (e.g. unresolved multiplets which result in significant resolution broadening should be avoided whenever possible).

If these lines are generated sequentially rather than simultaneously, care should be exercised to ensure that the counting rate is low and comparable; otherwise, count-rate induced gain shifts may be mistakenly interpreted as a pulse-height linearity problem. Also, care should be taken that equipment gain drifts are not mistakenly interpreted as non-linearities. The most reliable method is to generate all of the lines simultaneously.

Integral non-linearity (INL) is defined as the maximum deviation from linearity expressed as a percentage of the specified maximum linear output. When characterized by a single unqualified number, INL shall not exceed that number anywhere within the specified operation range of the instrument and shall be determined under the same conditions (instrument settings, etc.) used to specify resolution performance. The INL may be obtained from the previously described X-ray spectrum by plotting peak centre (modal) channel number for each peak versus the X-ray energy of that peak as shown in Figure 9, page 48

The ideal response curve is a straight line corresponding to a linear regression least squares fit to the data points with the same statistical weight for all measurements. The integral non-linearity, in per cent, is then defined by:

$$\mathrm{INL} = 100 \left(\frac{\Delta E_{\max}}{E_{\mathrm{F}}} \right) \tag{12}$$

where $\Delta E_{\max}$ is the maximum deviation (in energy units) between the measured and the ideal response, and E_{F} is the energy corresponding to the full scale of the energy range of interest.

8.2 *Integral linearity by the bridge method*

This measurement (supplementary method) is described in detail in Clause 21 of IEC Publication 340. It can be utilized only with detector systems that incorporate a pulser coupling capacitor as described in Sub-clause 7.1.

9. Count-rate effects

9.1 *Experimental arrangement*

Because most instruments which utilize gated baseline restoration do not tolerate the reverse polarity part of the pulse for a tail pulse generator or a square pulse generator, techniques which rely on a pulse generator to measure count-rate effects are frequently not useful for X-ray spectrometers.

The experimental arrangement for using a radioactive source to measure count-rate effects on spectral distortion is shown in Figure 10, page 49. The ^{55}Fe source shown in Figure 10 is located on the working axis of the detector, and the source to detector distance is varied to change the counting-rate. Generally, it is preferable that the radioactive source be sufficiently intense that the maximum desired counting-rate is obtained at a source to detector spacing not less than the standard working distance. If the source to detector spacing is too small, spectral distortions from edge effects in the detector may be misinterpreted as count-rate induced distortions. All extraneous scattering materials shall be kept well away from the space between or adjacent to the source and detector to eliminate spectral distortion by Compton scattered photons, or by secondary fluorescence X-rays. In general, it is preferable to use an X-ray source that does not produce any high energy events which would overload the amplifier. It is essential that the input stages of the ADC be d.c. coupled.

The equivalent input count-rate (r_{i}) is measured by the fast amplifier, discriminator, and counting ratemeter. In preamplifiers which utilize pulsed feedback, the r_{i} shown in Figure 10 does not represent the true input rate: to obtain the true input rate in this case a correction must be made for the dead time caused by the gated-off periods. In some cases, this correction may be very significant. The fast filter amplifier chain shall have a band-pass sufficient to ensure negligible counting losses or an accurate correction for the counting loss from pile-up must be applied. A good first-order correction is given by the relation:

$$r_0 = r_i \cdot e^{-r_i t_w} \tag{13}$$

where:

r_0 = unpiled-up output data rate
r_i = input data rate
t_w = width of the pulse (in seconds) at the baseline established by the discriminator threshold level

If the arrangement shown in Figure 10, page 49 is operated in the ungated mode (i.e., with the gate by-passed) the observed count-rate effects will include the contributions from the MCA. The contribution from the MCA (and gate) alone can be approximated in the following way:

Set the scaler overflow output to divide-by-one condition and the delay and the one-shot period long enough to gate the entire amplifier output pulse through the linear gate. Adjust the ^{55}Fe source position to produce the maximum desired counting-rate. Vary the counting-rate into the MCA by switching the scaler overflow output to ÷ 2, ÷ 4, ÷ 8, ÷ 16, ÷ 32, etc. The resulting shifts in resolution and peak shape can be attributed to the MCA and linear gate. The contribution from the linear gate can be minimized by using a good quality d.c. coupled linear gate.

Because of the derandomizing effect of the scaler, this technique will tend to underestimate the count-rate effects in the MCA at low and medium count-rates.

The main problems with count-rate effect measurements are:

a) the difficulty of isolating the contribution of any one component of the detector-preamplifier-amplifier-MCA system;

b) the dependence of count-rate performance on many factors, such as signal energy, preamplifier noise, and amplifier shaping time constants. It is therefore necessary, in specifying the system performance, that all the relative operating conditions be clearly stated, and that the system parameters are selected so as to approximate the conditions under which the system will be used. When investigating count-rate performance, it is imperative that the pole-zero cancellation networks and baseline restorers be properly adjusted.

When specifying system performance, the following shall be stated:

a) whether the results include the MCA effects;

b) energy range;

c) amplifier shaping time constants, including BLR setting and pile-up rejection;

d) low count-rate resolution;

e) energy at which the amplifier overloads;

f) radiation source and energy used for random signal source (preferred source is ^{55}Fe).

When specifying performance as a function of counting-rate, the counting-rate specified shall always be the counting-rate at the input (detector) of the spectrometer. The output counting-rate which corresponds to this input counting-rate shall also be stated.

9.2 *Pulse-height distribution peak shift*

The peak location (centroid) of a pulse-height distribution may exhibit dependence on total counting-rate. The experimental set-up shown in Figure 10, page 49, provides a means to measure pulse-height shift as a function of average counting-rate for random pulse spacing in time. The counting-rate is varied by adjusting the spacing between the radiation source and the detector and is measured with a count-rate meter. The Mn K_α peak should be set at 90% of the maximum specified linear output of the system. The counting-rate should then be varied over the entire range of interest, and the shift of the Mn K_α peak centroid plotted as a function of total input count-rate.

9.3 *Spectral resolution and line shape versus count-rate*

The set-up shown in Figure 10 is also used for this measurement.

The FWHM, FWTM, and peak-to-tail of the Mn K_α pulse-height distribution are measured for each of several counting-rates over the range of interest and tabulated or plotted as a function of input count-rate. The Mn K_α peak should be set as specified in Sub-clause 9.2.

9.4 *Counting losses*

At high counting-rates, pulse pile-up will cause a loss of counts from the peak as well as spectral distortion. In addition, systems which use gating techniques to eliminate spectral distortion or to effect pulsed feedback to the preamplifier will exhibit dead times during the gate closed periods. All systems are paralyzable; i.e., at some level of input count-rate, the output count-rate actually decreases with increasing input rate. Figure 11, page 50 illustrates this effect.

Either the arrangement shown in Figure 10 or that of Figure 12, page 51, may be used for this measurement. If the arrangement of Figure 10 is used, the counting-rate meter should be replaced with a counter-timer and the gain should be adjusted as in Sub-clause 9.2. If the arrangement in Figure 12 is used, the window widths in the fast single-channel analyzers should be set at six times the FWHM, and the centre of the window should correspond to the peak centre (modal point of the peak) at low count-rate. The arrangement shown in Figure 12 can be used only under situations where the pulse-height distribution peak shift with counting rate will not shift the peak out of the window of the SCA. The fast filter amplifier chain shall have a band-pass sufficient to ensure negligible counting losses, although a small calculated dead-time loss correction for the fast filter amplifier chain may be required.

The count-rate is increased by decreasing the source-to-detector distance, and the counting-rate of the analyzed pulses in the X-ray peak is plotted as a function of total count-rate in the fast filter amplifier chain as shown in Figure 13, page 52. The results of Figure 11 can be derived from those of Figure 13.

Counting loss effects which are attributable to the MCA may be measured by disabling the coincidence gate input shown in Figure 10, page 49 (as described in Sub-clause 9.1).

The arrangements of Figure 10 or 12, page 51 can also be used to verify dead time corrections.

10. Overload effects

10.1 *General*

The behaviour of an amplifier receiving an input pulse that drives the amplifier far into the overload region depends on many factors. The order in which different sections of the amplifier overload as the input amplitude is increased may depend on the gain control and time constant settings. All of the gain control settings and pulse-shape parameters shall be stated when the overload recovery time is specified; otherwise, the specification shall apply for all gain and filter network combinations available in the system. Amplifiers having adjustable pole-zero cancellation and baseline restoration networks must be properly adjusted before overload tests are performed.

10.2 *Amplifier gain recovery time*

A system is defined as having recovered from overload when the output waveform returns to and remains within a band about the baseline of 1% of the maximum specified output voltage, and when the gain for small signals has returned to normal. After an overload pulse, the output waveform of some amplifiers returns to the baseline sooner than the gain returns to normal. Return to normal gain may usually be judged by the reappearance of full noise or small signal response on the oscilloscope trace. The test arrangement shown in Figure 5, page 45 permits a quick measurement of recovery time after an overloading pulse. If the pulse generator is replaced with a sine-wave generator, working at low signal level, the reappearance of the sine wave can be used instead of the noise.

An example of such overload behaviour is illustrated in Figure 14, page 52. Note that the small sinusoidal signal on the trace reappears when the amplifier gain has returned to normal. The waveform returns to the baseline very quickly after the overload pulse, but the gain does not recover until much later. Oscilloscope overload must be avoided. Amplifier gain recovery time shall be stated for overload factors of 10, 100, and 1 000 at all relevant time-constant and gain settings.

11. Pulse-height stability

11.1 *Line voltage variations*

The test set-up is identical with that shown in Figure 5 except that the line voltage is variable for all parts of the system except the precision pulse generator, multichannel analyzer, and oscilloscope. A pulse generator peak and/or a peak from a monoenergetic X-ray line (e.g. ^{55}Fe) may be used to measure stability.

Set the line voltage at its nominal value and adjust the amplifier output so that the peak centre (modal) channel of the peak N_l is at 90% of full scale on the MCA. Observe the maximum deviation of N_l as the line voltage is varied over a range of 88% to 110% of the nominal operating voltage while all other conditions are maintained constant. This variation is often expressed in percentage for a given line voltage change and is obtained by the relation:

$$S_L = \frac{100\,\Delta N_l}{N_l} \tag{14}$$

A similar test may be performed with a biased amplifier in the system. In this case, the pulse generator and gains should be adjusted to give 90% of maximum rated output voltage from the biased amplifier at the desired gain and bias level setting. Spectra should be obtained at 88% and 110% of nominal line voltage. Output pulse height stability S_L (pulse-height variation over a +10%, −12% line voltage range) is given in per cent by:

$$S_L = 100\,\frac{\Delta N_l}{N_l + G_B N_B} \tag{15}$$

where ΔN_l is the number of channels between the peak centre (modal) channels of the peaks, G_B the gain of the biased amplifier and N_B is the equivalent number of channels suppressed by the biased amplifier. Measurement of the effect of the MCA on pulse-height stability can be accomplished by repeating the above with variable line voltage to the MCA only.

11.2 *Temperature effects*

For this test, the system shown in Figure 5, page 45, (except for the pulse generator, MCA, and oscilloscope) is placed in an environmental test chamber. The maximum change in pulse height produced by incremental changes of the ambient air temperature, with other conditions maintained constant, is the temperature coefficient of pulse height; for example, 0.01% per Kelvin.

In amplifiers with d.c. coupling, pulse-height shifts can be caused by either gain changes or d.c. level shifts. When applicable, temperature induced pulse-height changes in both gain and d.c. level shall be measured and specified. When specifying the temperature coefficient of pulse height, the range over which the specification applies shall be clearly stated. The measurements shall be made over a specified temperature range and taken at no greater than 10 K increments. The specified temperature coefficient shall be valid for all increments within the specified temperature range. Care should be taken not to damage the system by operating outside the manufacturer's recommended operating temperature range.

11.3 *Gain stability*

The test set-up is identical with that shown in Figure 5 and Sub-clause 11.1. Gain variations can be determined by observing the peak centre (modal) channel shift in the MCA. Test conditions should be maintained constant and the maximum gain variations noted over an extended period of time which shall be stated.

12. Efficiency

The efficiency of a semiconductor detector at a given photon energy is a function of a number of variables including the area, shape and depth of the active region, the presence of collimators, and the absorption in windows (or dead layers) between the source of X-rays and the active region. In addition, the presence of nearby extraneous scattering material can also bias the accuracy of efficiency measurement. In specifying the efficiency of the detector, it is also essential that the active area be specified.

Since the periphery of the sensitive region is usually a charge collection problem area, many semiconductor X-ray spectrometers are constructed with internal collimation. Any description or specification of the active area of the detector should unambiguously specify the dimensions, shape, Z, and location of collimators. Other regions of low electric field in the device may also cause spectral distortions; therefore, in specifying the sensitive depth of the detector, the thickness of any non-depleted material shall be clearly stated.

12.1 *Window attenuation measurements with glass fluorescent source (preferred method for instruments intended for use below 5 keV)*

In this measurement, the ratios of the relative intensities of fluoresced X-rays from a standard glass with composition as in Table I are used to quantify the attenuation in the cryostat window and the detector dead layer.

The standard glass shall be excited by ^{55}Fe as illustrated in Figure 15, page 53. The resulting X-ray spectrum obtained with the arrangement of Figure 5, page 45, is used to characterize the window attenuation.

Since the relative intensities of the fluorescent X-ray lines incident on the detector window are affected by absorption in the glass target, this measurement is sensitive to the source-glass-detector geometry. The geometric arrangement shown in Figure 15 has been selected to minimize the effect of small variations in the dimensions, while still maintaining a reasonable counting rate. With the geometry shown in Figure 15 and a $1.9 \cdot 10^9$ Bq (50 mCi) ^{55}Fe source, the data shown in Figure 16, page 54, (with 400 000 counts in the Mn K_α peak) can be obtained in about 5 h. Any portion of the structure, except the glass target, which could emit interfering secondary X-rays shall be shielded from the detector with plastic. Plastics containing catalysts or fillers which emit interfering X-rays shall be avoided.

The typical spectrum shown in Figure 16a, page 54, was obtained using a Si (Li) detector in a cryostat with an 8 μm thick Be window. Figure 16b, page 54, shows the effect of interposing an additional 124 μm thick Be absorber. The indices of interest are the intensities of the low-energy lines relative to the intensity of the coherently backscattered Mn K_α line.

The composition of the standard glass is as in Table I.

TABLE I

Composition of standard glass

(Percentage of weight)

SiO_2	42.5	MgO	20.0
BaO	2.0	ZnO	20.0
CaO	1.5	B_2O_3	10.0
Li_2O	4.0		

Fluorescence of the standard glass with a ^{55}Fe source produces the prominent lines shown in Table II.

TABLE II

Characteristic X-ray lines from the standard glass fluoresced by ^{55}Fe source

Mn,	K_α	5.90 keV (coherent backscatter)
Ba,	$L_{\alpha1}$	4.47, $L_{\alpha2}$ – 4.45, $L_{\beta1}$ – 4.83; $L_{\beta2}$ – 5.16; L_γ – 5.53
Ca,	K_α	3.69, K_β – 4.01, L – 0.34
Si,	K_α	1.74, K_β – 1.83
Mg,	K_α	1.25, K_β – 1.30
Zn,	L_α	1.01, L_β – 1.03
O,	K_α	0.523
B,	K_α	0.185 keV

Figure 16a, page 54, clearly shows Mn, Ca, Si and Mg lines, while the Zn-L line is barely detectable above the background.

The window index (W_E) at a given energy (E) is defined by the relationship:

$$W_E = \frac{A_E}{A_{\mathrm{Mn}}} \qquad (16)$$

where A_E is the total number of counts in the peak at energy E, and A_{Mn} is the intensity of the backscattered Mn K_α line. The procedure for determining A from a spectrum such as Figure 16, page 54, is described at the end of this sub-clause.

Frequently, a single value for W_E will adequately characterize the drop in efficiency at low energies. However, additional useful information about the origin of the window attenuations can sometimes be obtained by comparing values of W_E at several energies. When an instrument is characterized by a single W_E it should correspond to the lowest energy line which will provide data of reliable statistical accuracy. Lines with line-to-background ratios of less than 3 should normally not be used. If the propagation of statistical errors in the determination of W_E exceeds ±3% at the 90% confidence level, then the probable error (90% confidence limit) in the value of W_E shall also be specified.

Typical values of W_E for the example shown in Figure 16, are illustrated in Figure 17, page 55 , which is included here only for the purpose of illustrating the sensitivity of this technique.

The procedures described in this sub-clause are also useful for "windowless" detectors where the vacuum-tight barrier between the detector and source of X-rays is removed during operation. In this case, care must be exercised to ensure that the detector and/or preamplifier are not damaged by poor quality of the vacuum in the vicinity of the X-ray fluorescent source.

The method for peak area and spectral background subtraction has been chosen for its simplicity and ease of computation, although in certain circumstances, such as in the presence of seriously distorted spectral peaks, the method could yield misleading results.

For the analyses described below, a spectral peak shall be at least six channels wide at half-maximum and the total number of counts within the FWHM shall be at least 10 000. If computer fitting of the data is used, the 10 000 counts minimum need not apply, provided the result as calculated by computer is accurate to within ±3% (90% confidence level).

Pulse-height spectral data should be plotted as the log of the number of counts N_x in the channel x versus channel number X. On this plot, background under the X-ray peaks is determined by a linear fit to the average backgrounds on the upper and lower energy sides of the peaks of interest (see line B_1B_2 of Figure 18, page 56) The counts within the peaks are determined as those above this background line up to clearly defined minima between adjoining peaks. Background and peak definitions are shown in Figure 18. Peaks not clearly defined shall not be used; peak-to-valley ratio shall be not less than 10.

12.2 *Window attenuation measurement with radioactive sources*

Some detectors not intended for operation below 6 keV may have a dead layer or window which is too thick to allow use of the techniques of Sub-clause 12.1. In this case, a similar procedure which employs a radioactive source with two or more lines whose relative intensities are well known can be used to specify W_E. The intensity of the higher energy line is the denominator in equation 16. The detector shall be thick enough to totally absorb the higher energy X-ray. For this measurement, the glass target and the ^{55}Fe source are replaced by the appropriate radioactive source located on the working axis of the detector at the specified working distance.

For example, if ^{109}Cd is used, the detector sensitive region shall be thick enough to totally absorb the 88 keV X-rays and the window thickness index is given by the ratio of A_{22} over A_{88}. For cases where the source has more than two characteristic lines care shall be taken to clearly specify which two lines are used to determine W_E. Care shall be taken also to ensure that self-absorption in the source and its housing is negligible.

Typical sources which are useful for this measurement are listed in Table III.

TABLE III

Radioactive sources for characterizing window thickness

Radioactive source	Energy (keV)	Probability per decay
^{57}Co	6.4	0.494 ± 0.015
	14.4	0.0954 ± 0.0013
	122.0	0.866 ± 0.019
	136.0	0.1061 ± 0.0018
^{109}Cd	22.1	0.842 ± 0.028
	88.0	0.0373 ± 0.0006
^{133}Ba	30.9	0.969 ± 0.02
	35.0	0.226 ± 0.006
	53.2	0.0217 ± 0.0004
	81.0	0.335 ± 0.005
	161.0*	0.0062 ± 0.0004
^{125}I	27.2	0.398 ± 0.014
	27.5	0.742 ± 0.025
	31.0**	0.258 ± 0.010
	35.5	0.0667 ± 0.0022

* Avoid the use of the 161 keV line of ^{133}Ba as a reference peak because of interference from sum peaks.

** Average of K_β lines.

12.3 *High energy efficiency measurements*

The drop in efficiency at high energies is a function of detector sensitive depth and diameter, the Z of the semiconductor, and the details of the collimation. The easiest way to measure most of these parameters is by direct physical measurement before the system is assembled.

In addition, the sensitive depth of the detector element can usually be estimated by the capacitance (voltage characteristics of the diode before it is assembled with the preamp). Some verification of these parameters may be obtained by measuring the absolute efficiency at one or more appropriate energies. Additional information may sometimes also be obtained by measuring the efficiency as a function of source to detector spacing. In these types of measurement, care should be taken to avoid the presence of extraneous scattering material that might scatter photons into the detector.

In attempting to interpret these types of measurements, it is essential to know the relevant dimensions, positioning, and Z of the collimators since the collimators may not be totally effective at high energies.

If the detector element is not totally depleted, then its efficiency will be a function of detector bias voltage for X-ray energies which are not totally absorbed by the sensitive region.

Some available standard sources which are useful for absolute efficiency measurements are listed in Table IV.

TABLE IV

Standard sources for efficiency measurements

Source	Half-life	Energy (keV)	Probability per decay
^{55}Fe (Mn K_α, K_β)	2.7 yrs	5.89	0.082 ± 0.007
		5.90	0.163 ± 0.012
		6.49	0.033 ± 0.003
^{125}I	60.1 days	27.2	0.398 ± 0.014
		27.5	0.742 ± 0.025
		31.0	0.258 ± 0.010
		35.5	0.0667 ± 0.0022
^{109}Cd	464 days	22.1	0.842 ± 0.028
		24.9	0.0604 ± 0.0023
		88.0	0.0373 ± 0.0006
^{152}Eu	13.3 yrs	121.8	0.2838 ± 0.0023
		244.7	0.0751 ± 0.0007
		344.3	0.2658 ± 0.0019
		411.1	0.02233 ± 0.000 13
		444.0	0.03179 ± 0.000 45
		779.0	0.1296 ± 0.0007
		964.0	0.1452 ± 0.0006
		1 086.0	0.1016 ± 0.0005
		1 112.0	0.1356 ± 0.0006
		1 408.0	0.2085 ± 0.0009
^{60}Co	5.27 yrs	1 173.2	0.999 00 ± 0.000 20
		1 332.5	0.999 824 ± 0.000 005
^{133}Ba	10.74 yrs	30.9	0.969 ± 0.020
		35.0	0.226 ± 0.006
		53.2	0.0217 ± 0.0004
		81.0	0.335 ± 0.005
		276.4	0.0709 ± 0.0013
		302.9	0.1840 ± 0.0020
		356.0	0.621 ± 0.007
		383.9	0.0891 ± 0.0010

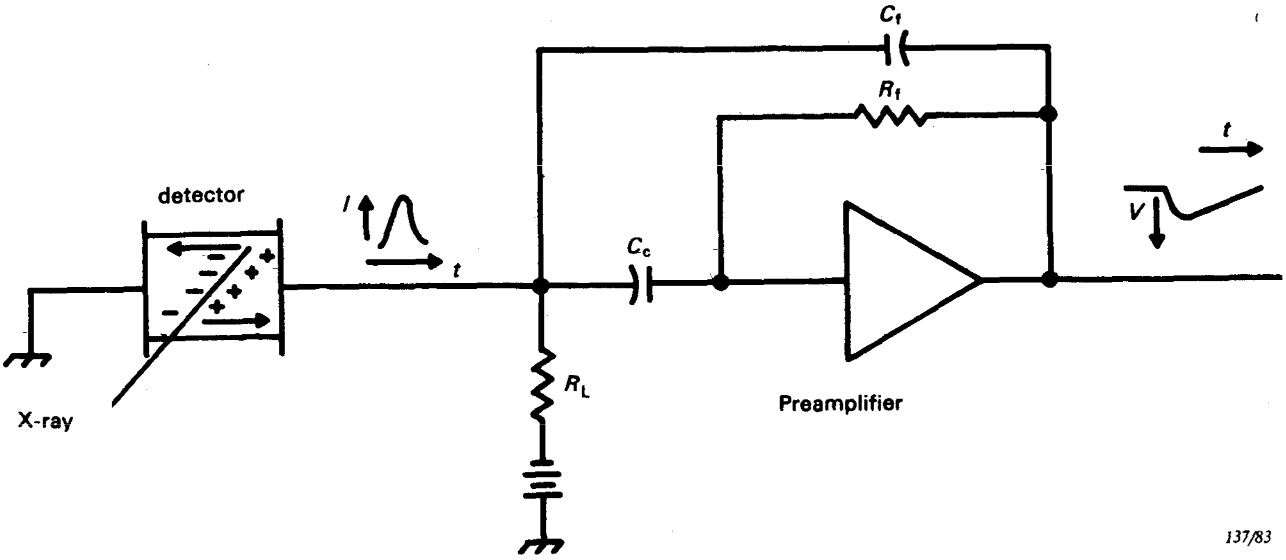

FIG. 1a. — A.C.-coupled configuration.

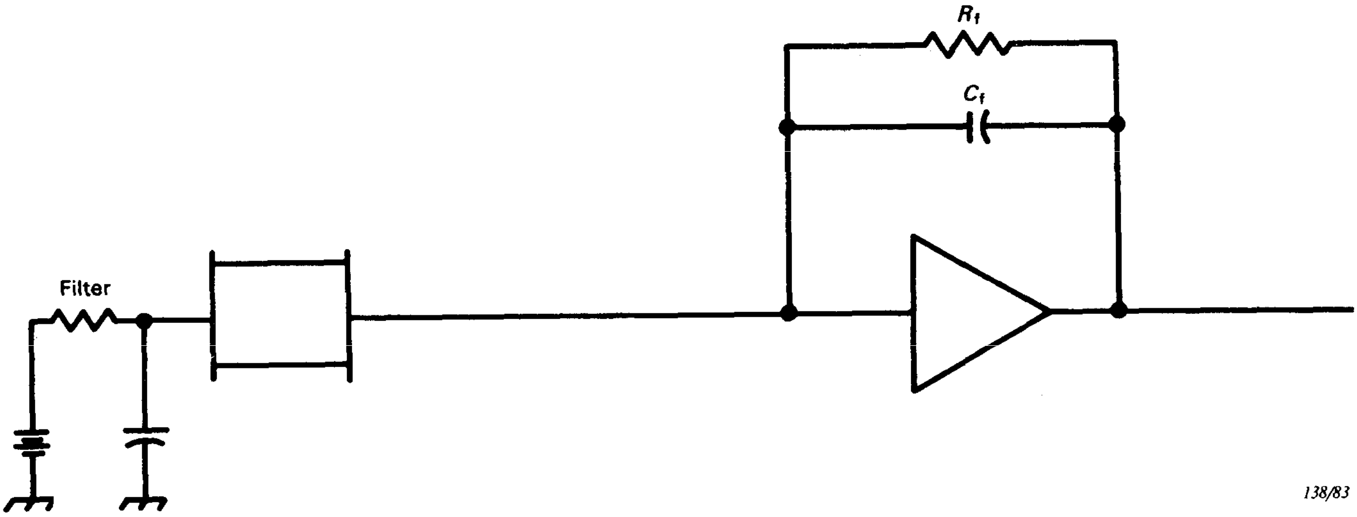

FIG. 1b. — D.C.-coupled configuration.

FIG. 1. — Schematic of semiconductor detector and preamplifier.

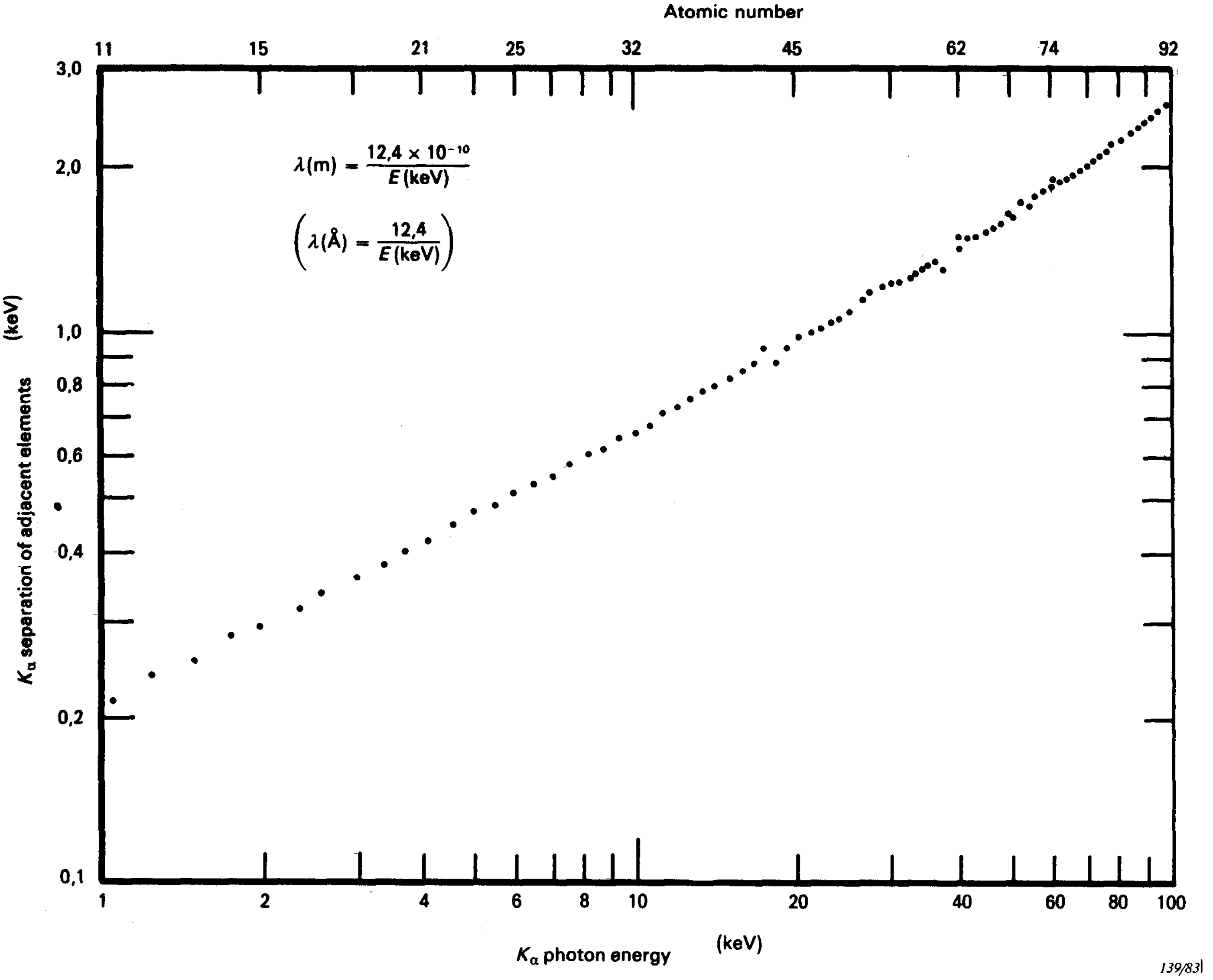

FIG. 2. — Spectral line separation as a function of energy and atomic number.

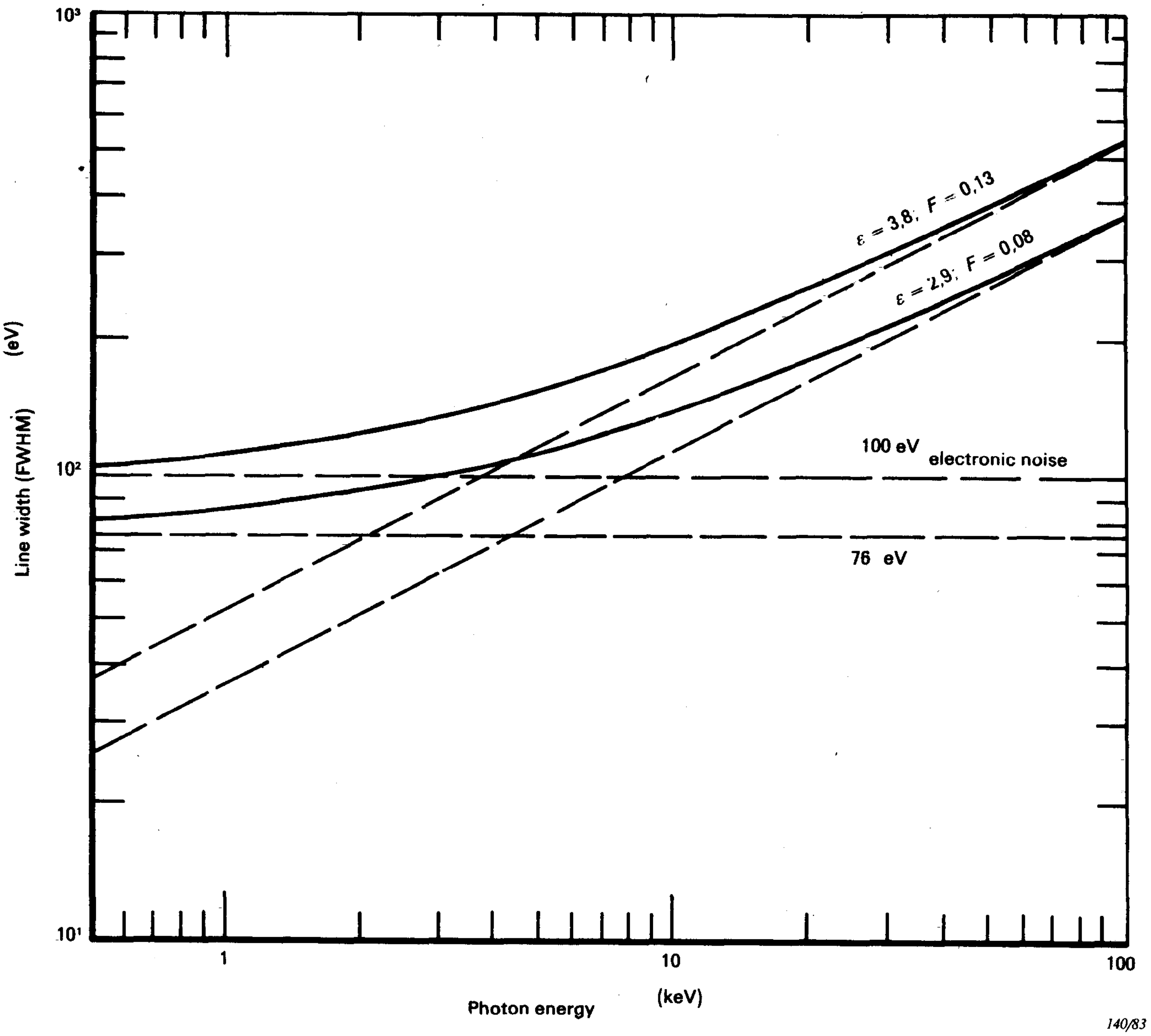

FIG. 3. — X-ray energy line width as a function of energy for several values of electronic noise and Fano factor.

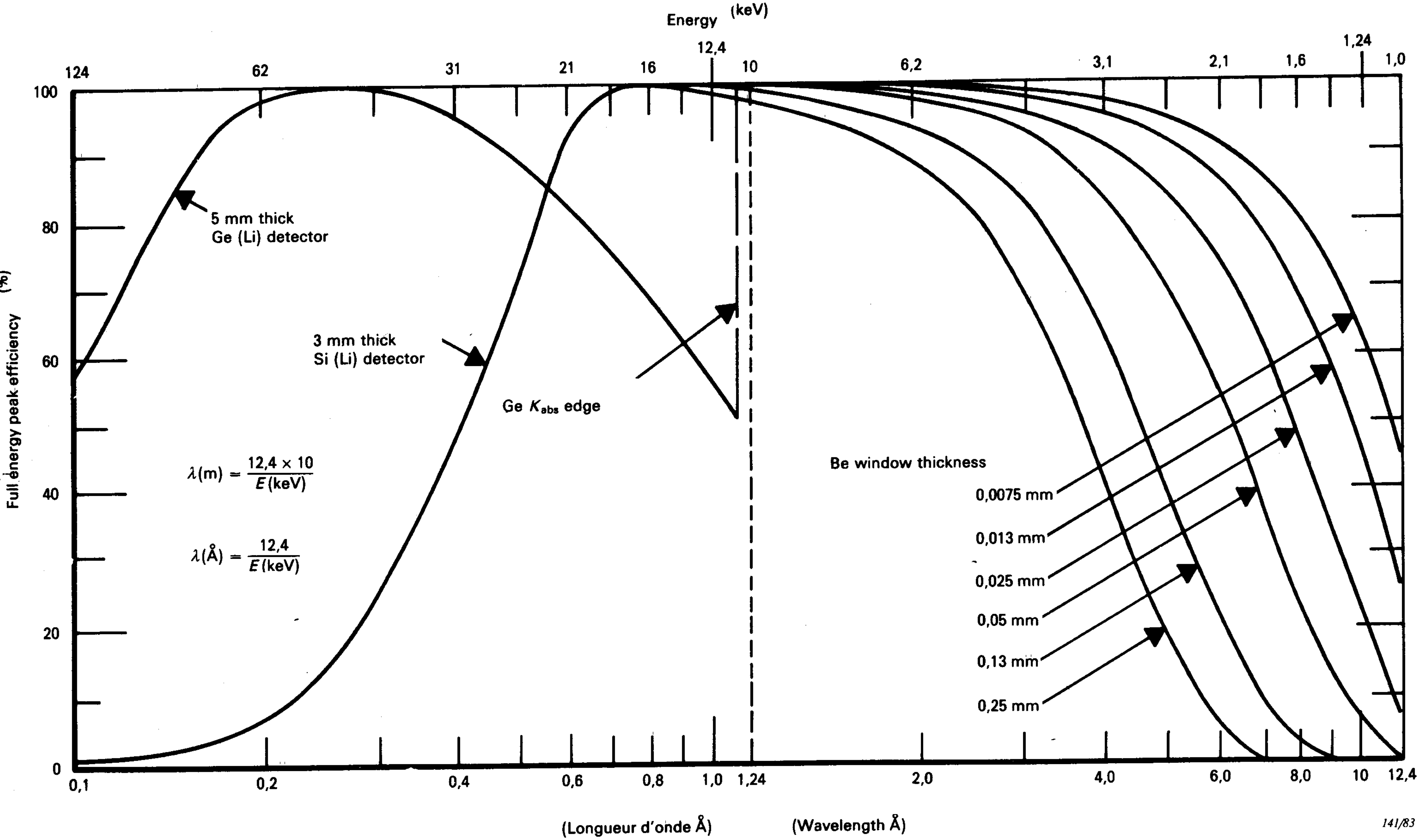

FIG. 4. — Full-energy peak efficiency versus energy for several X-ray energy spectrometers.

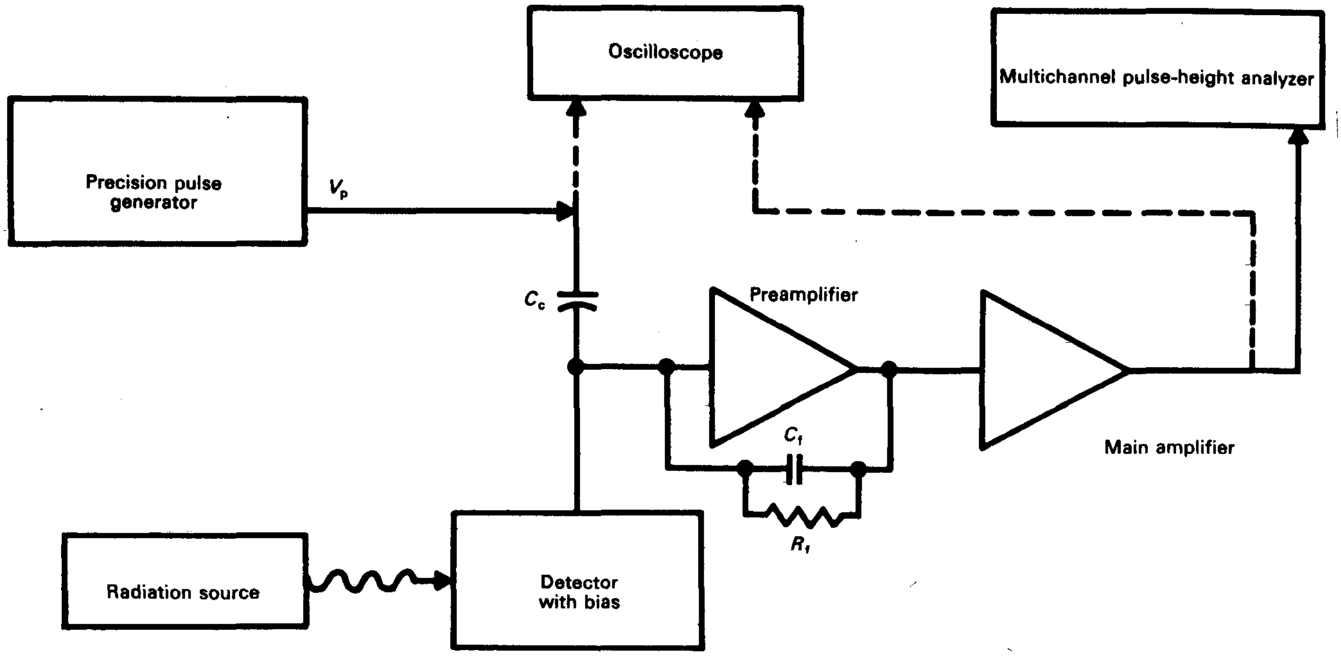

FIG. 5. — Measurement of pulse-height distribution.

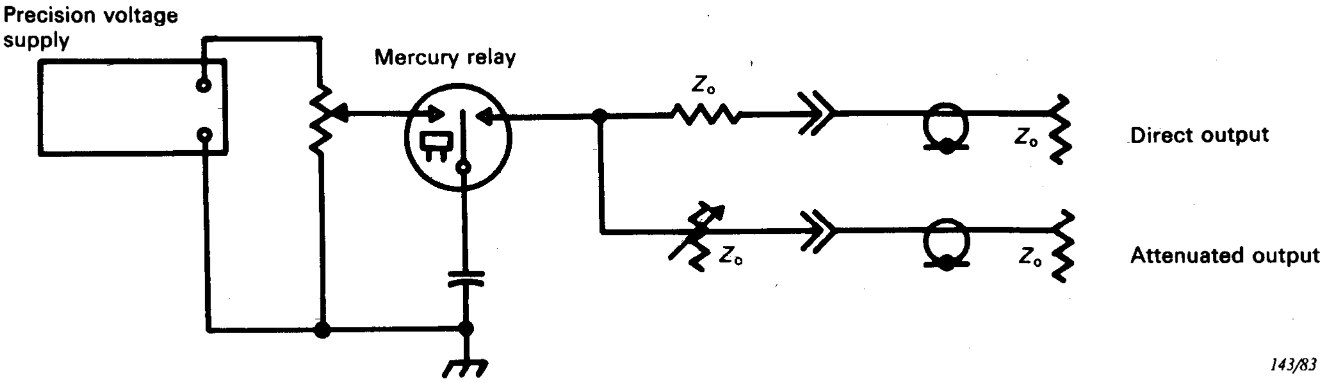

FIG. 6a. — Precision pulse generator.

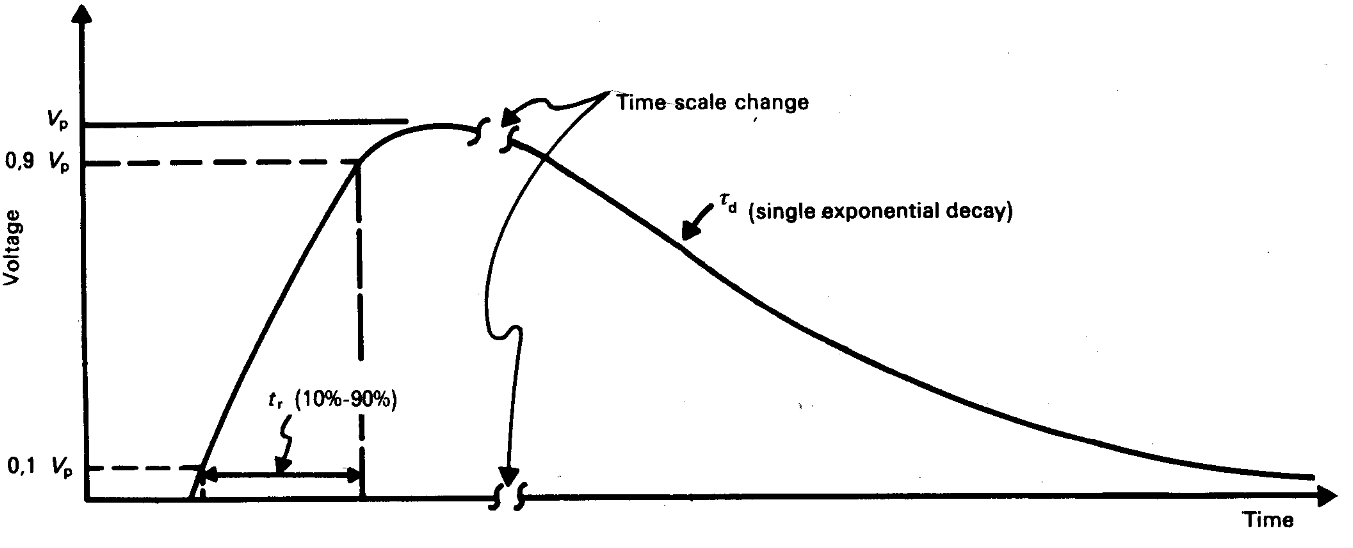

FIG. 6b. — Waveform.

FIG. 6. — Precision pulse generator and waveform.

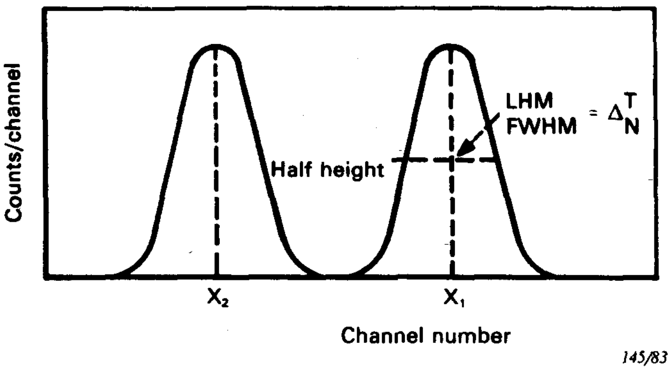

FIG. 7. — Typical noise measurement pulse-height spectrum.

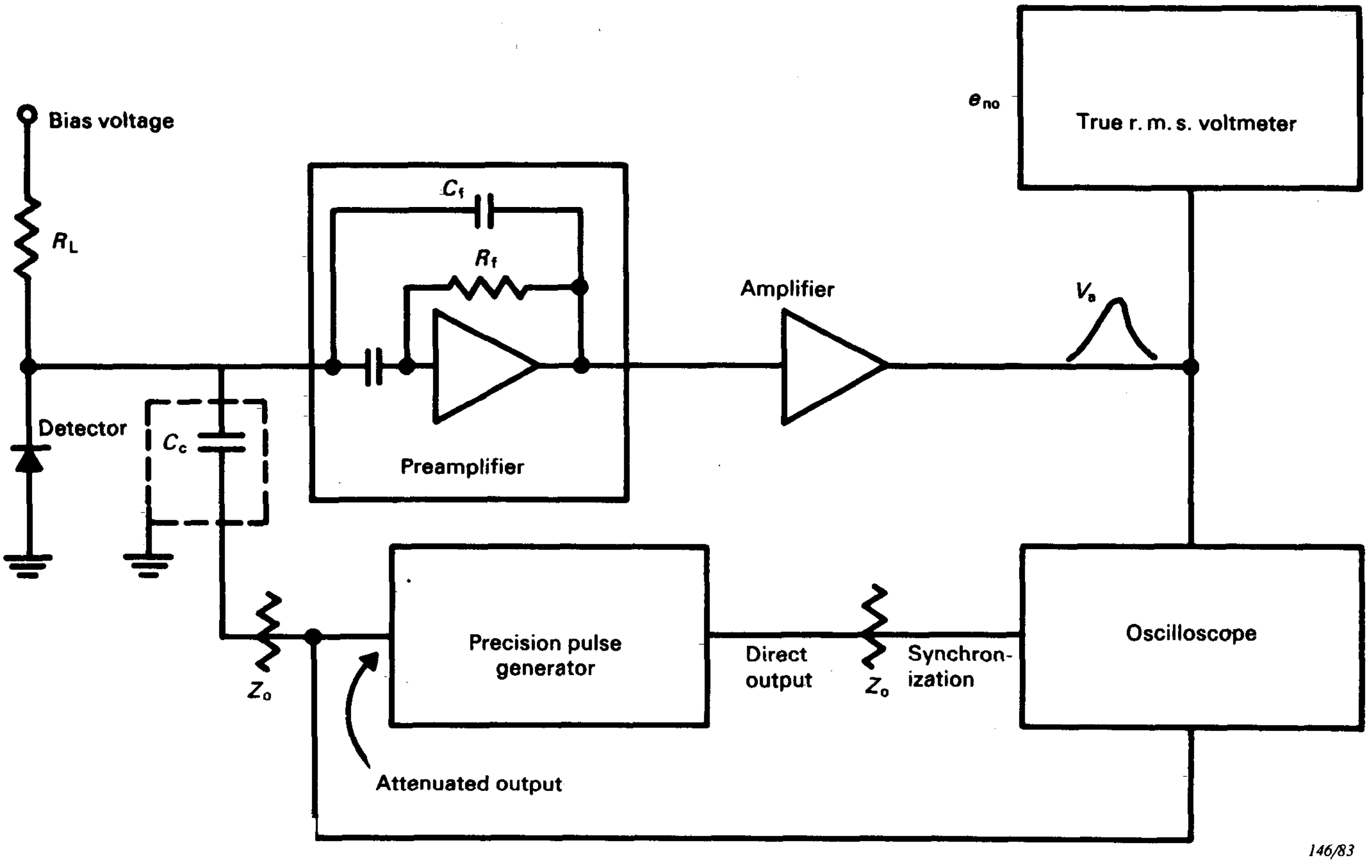

FIG. 8. — Noise measurement by oscilloscope and true root-mean-square voltmeter.

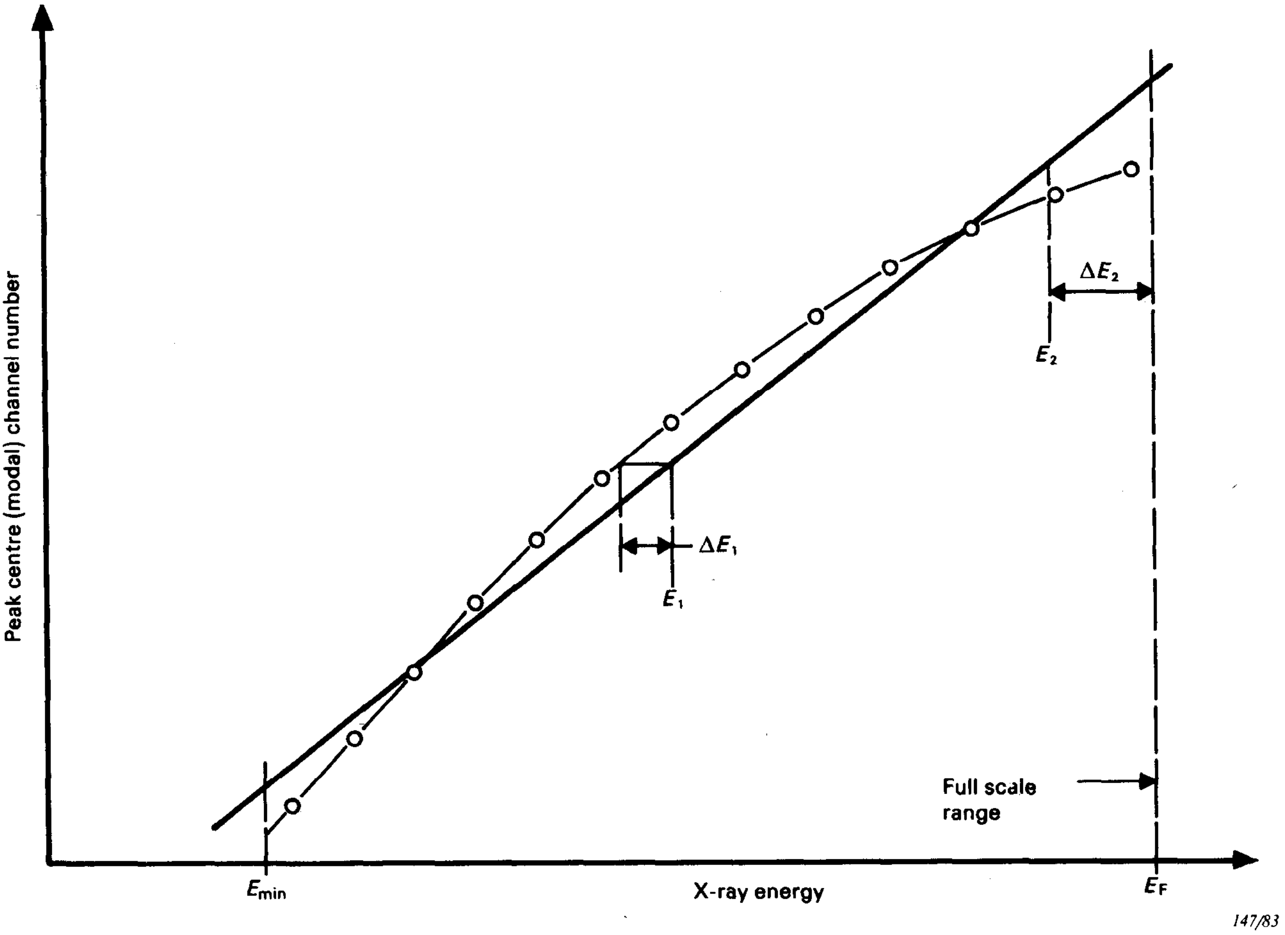

FIG. 9. — Measurement and display of linearity.

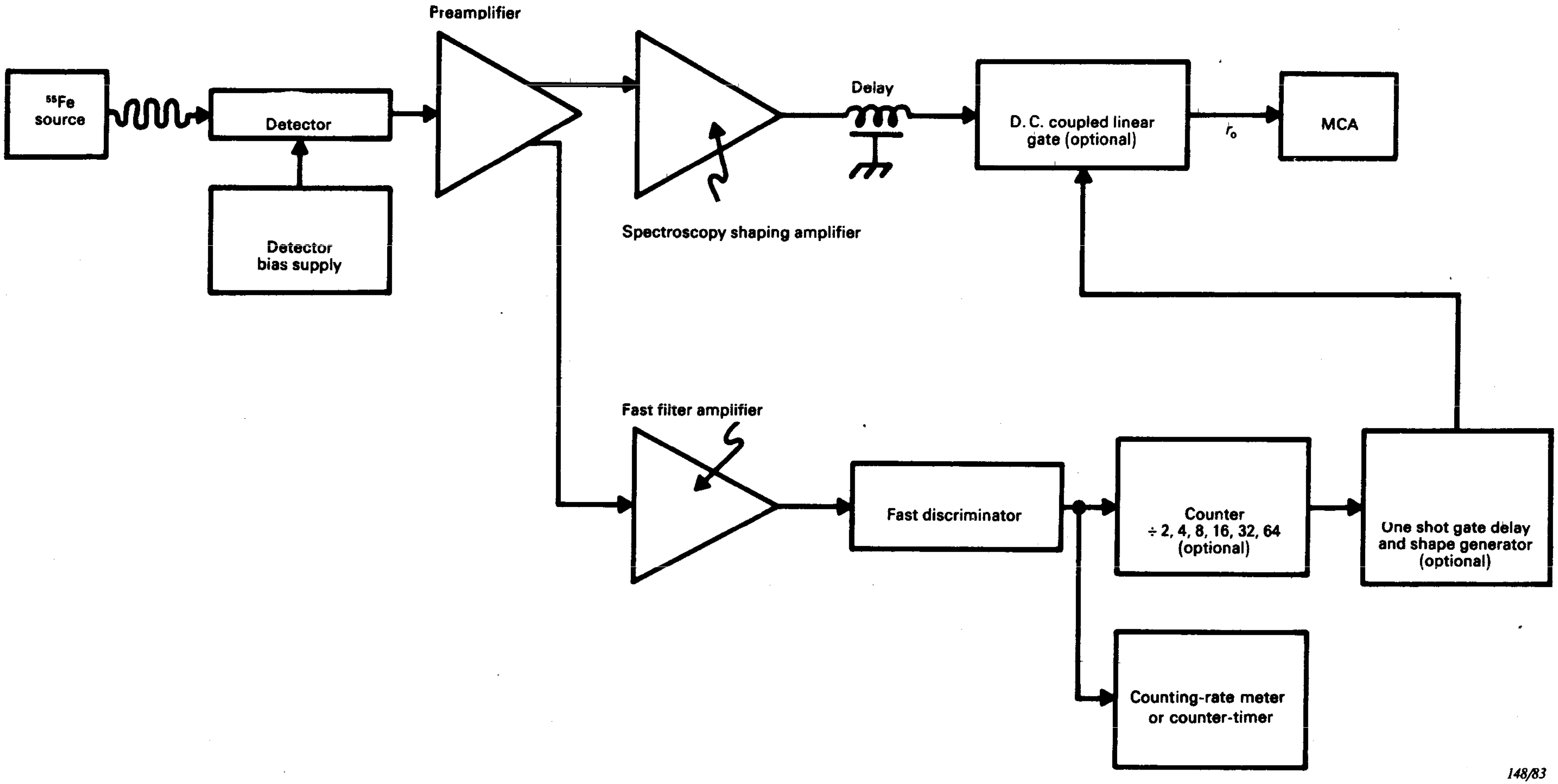
Preamplifier
^{55}Fe source
Detector
Detector bias supply
Spectroscopy shaping amplifier
Delay
D. C. coupled linear gate (optional)
r_o
MCA
Fast filter amplifier
Fast discriminator
Counter ÷ 2, 4, 8, 16, 32, 64 (optional)
One shot gate delay and shape generator (optional)
Counting-rate meter or counter-timer
148/83

FIG. 10. — Experimental set-up using multichannel analyzer to measure spectral distortion resulting from counting-rate effects.

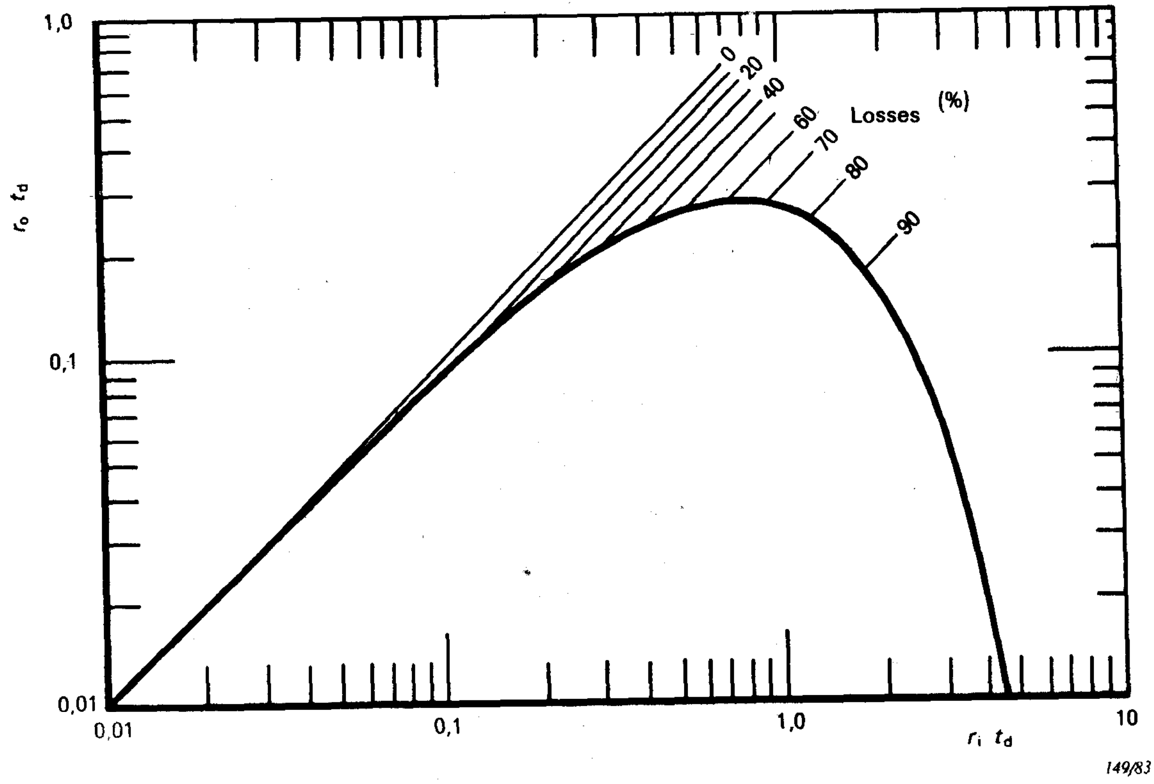

FIG. 11. — Output rate r_o versus input rate r_i for a paralyzable system with a dead-time t_d.

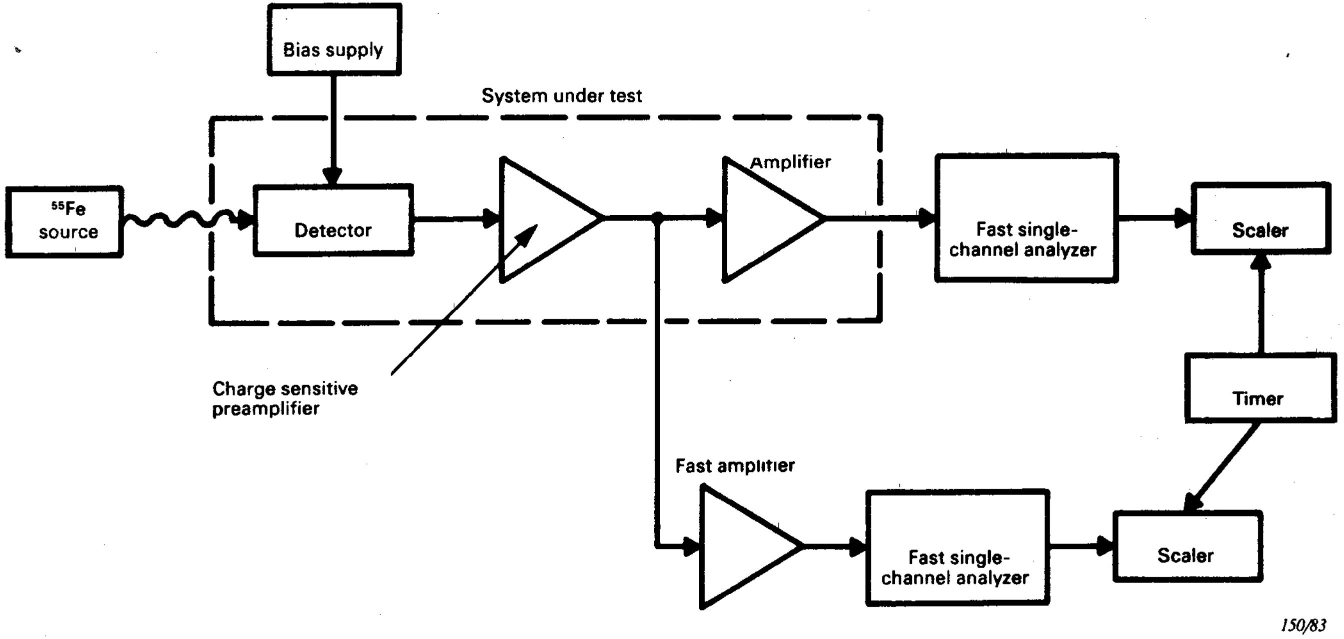

FIG. 12. — Experimental arrangement using single-channel analyzers to measure counting losses.

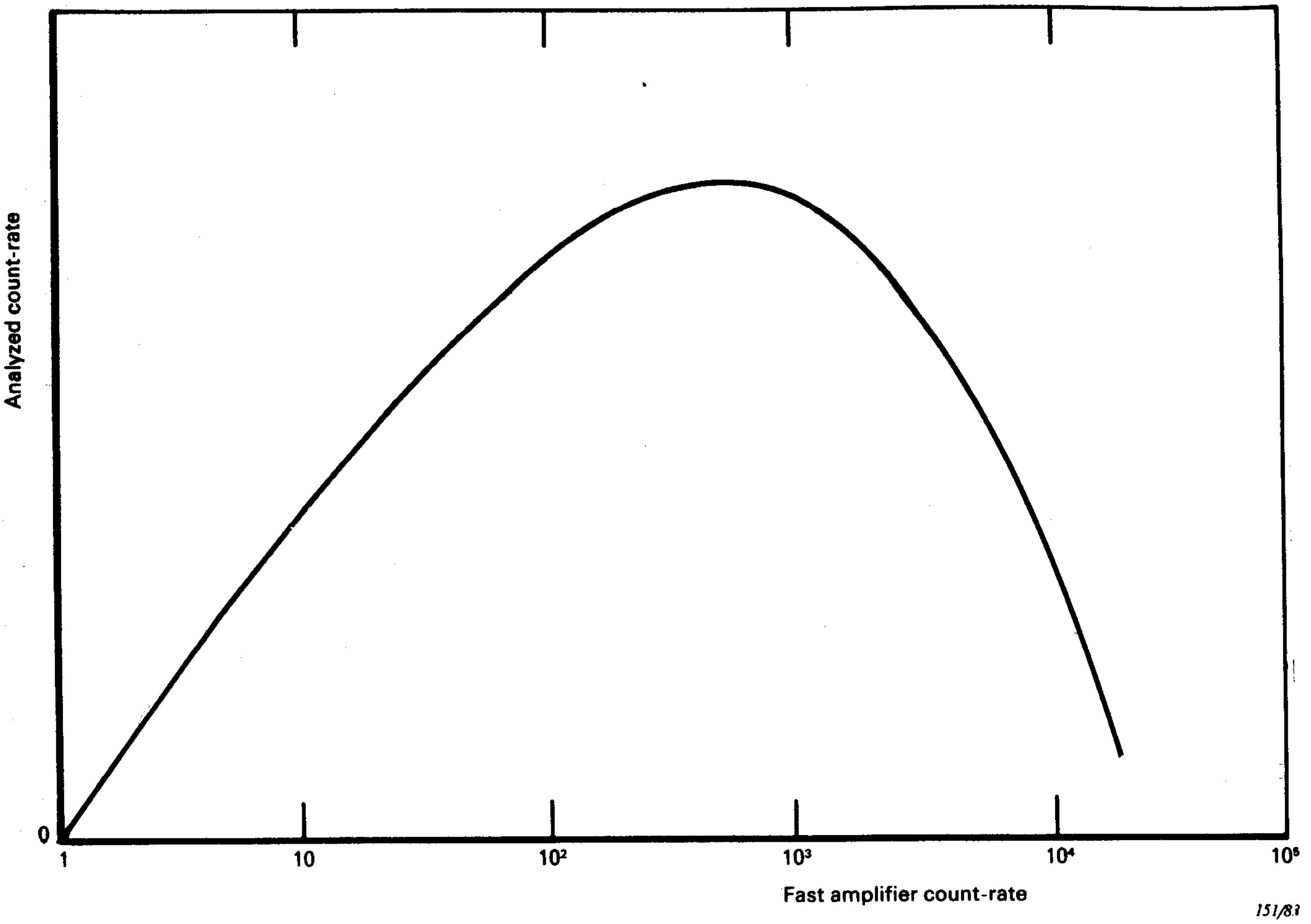

FIG. 13. — Analyzed count-rate in Mn K_α and K_β peaks as a function of the count-rate from a fast amplifier.

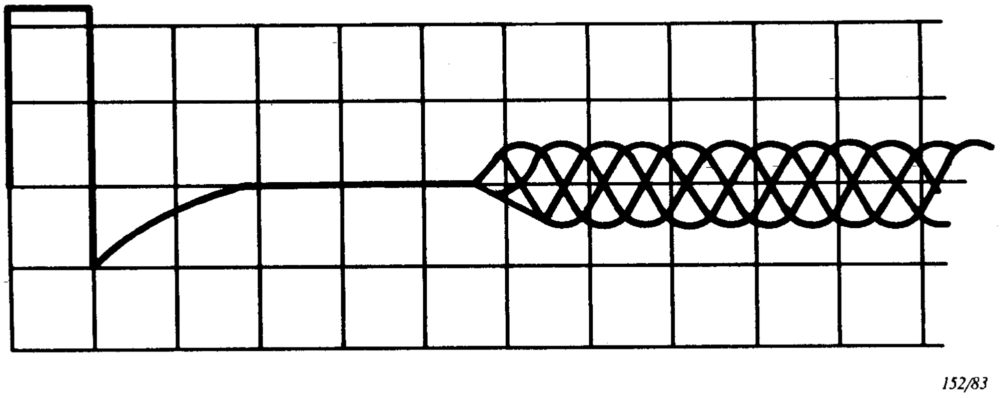

FIG. 14. — Example of gain recovery after overloading pulse.

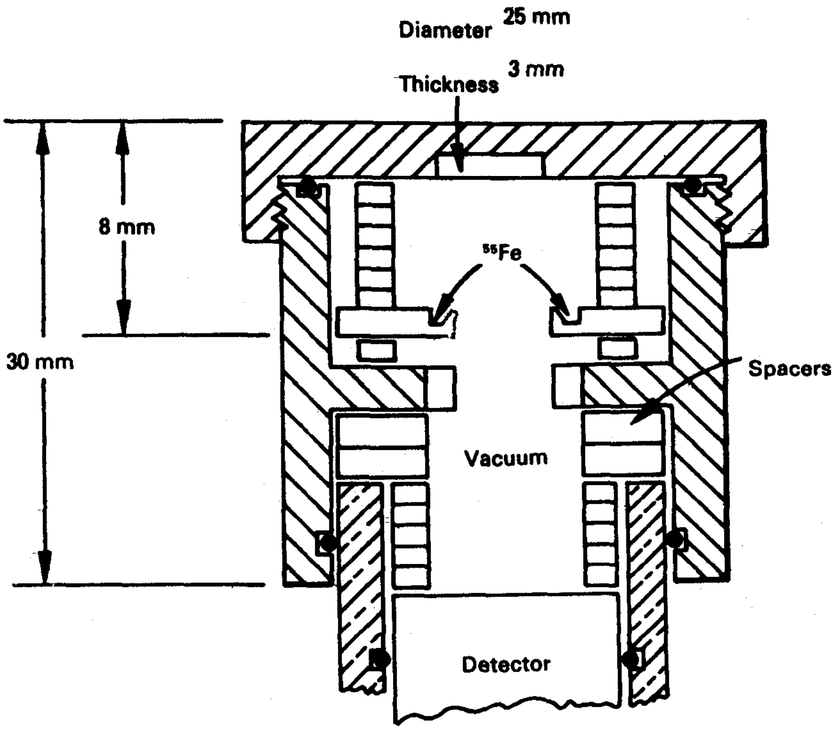

FIG. 15a. — Apparatus for window thickness measurements.

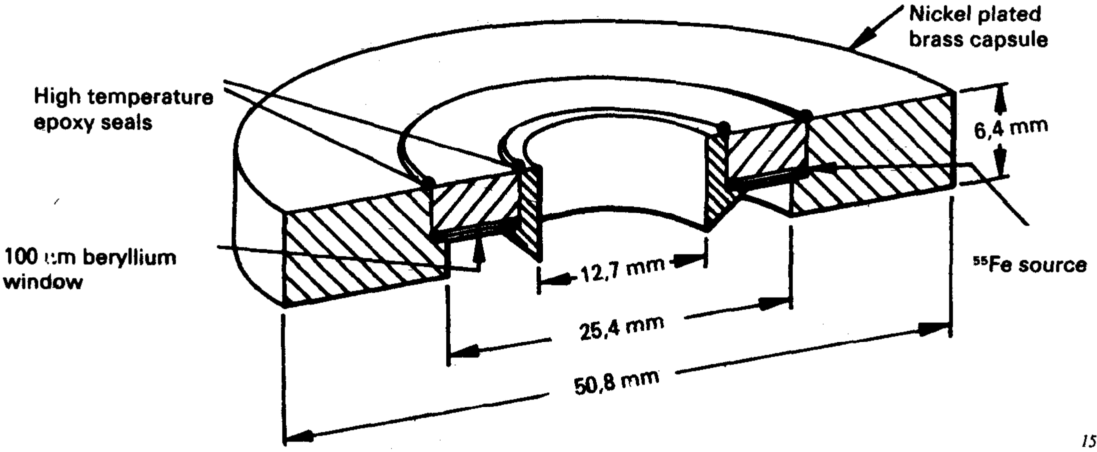

FIG. 15b. — Annular ^{55}Fe X-ray source

FIG. 15. — Fluorescent X-ray source assembly for window thickness measurements.

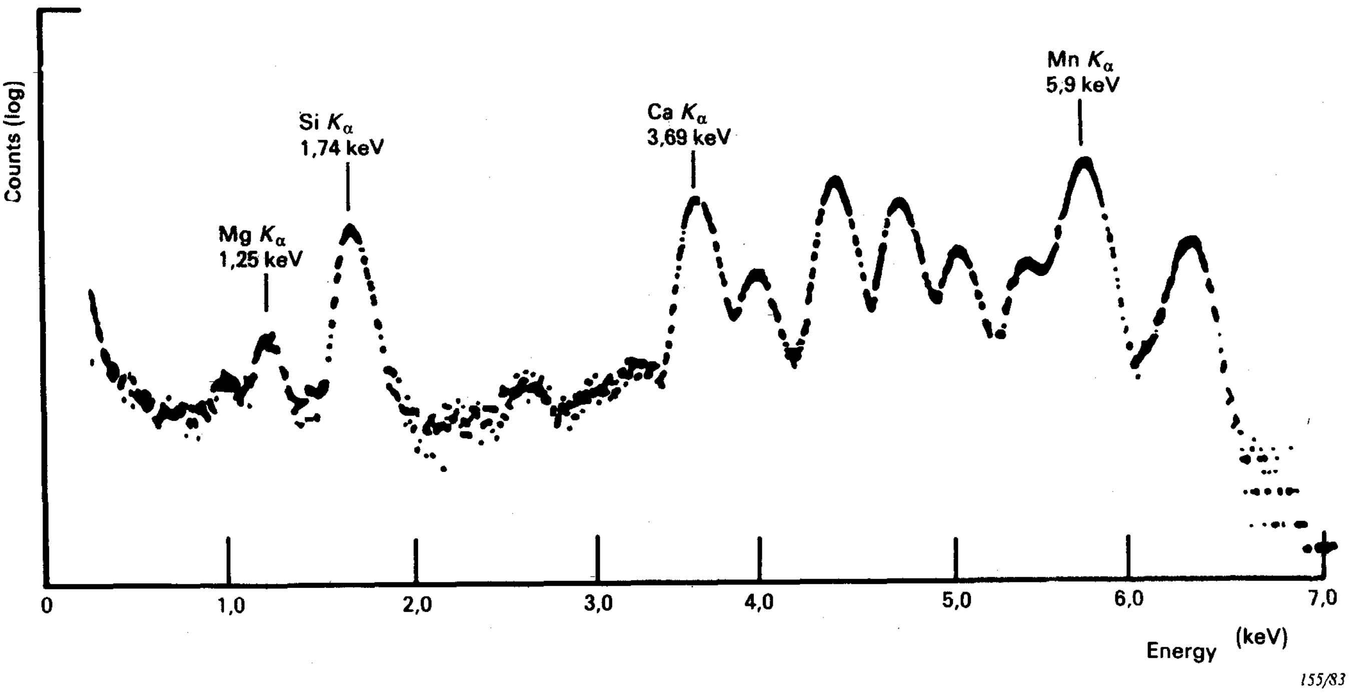

FIG. 16a. — Spectrum obtained with an 8 µm beryllium window.

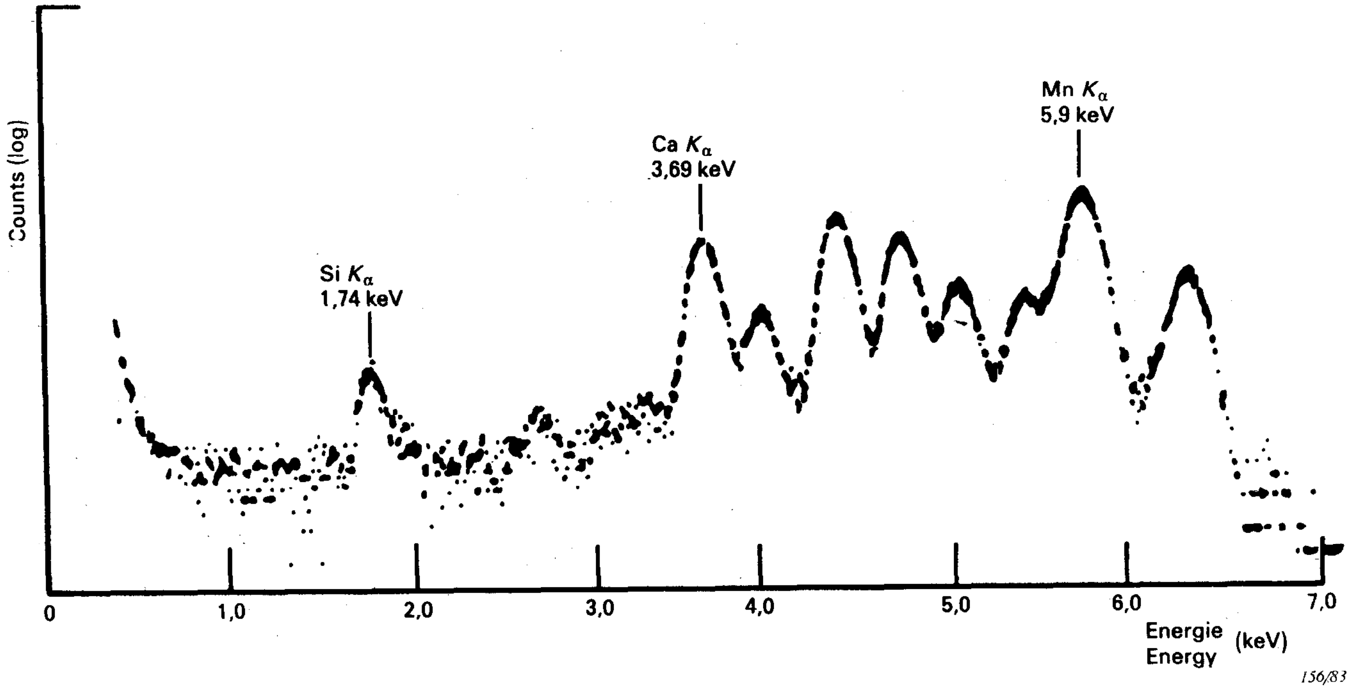

FIG. 16b. — Spectrum obtained with a 132 µm beryllium window.

FIG. 16. — Typical Si detector spectra for ^{55}Fe-excited standard glass.

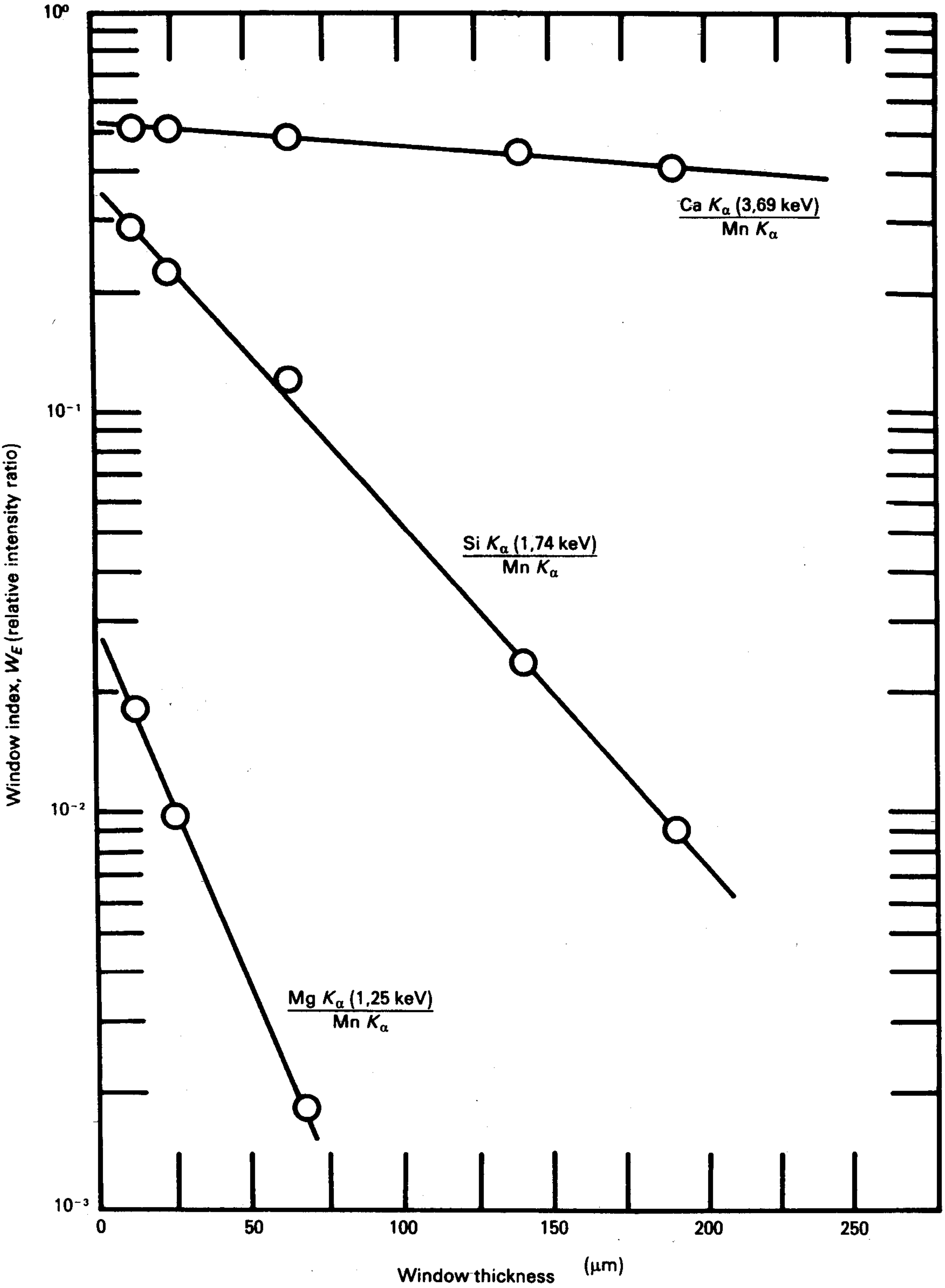

FIG. 17. — Typical behaviour of the window index, W_E, as a function of window thickness at several energies.

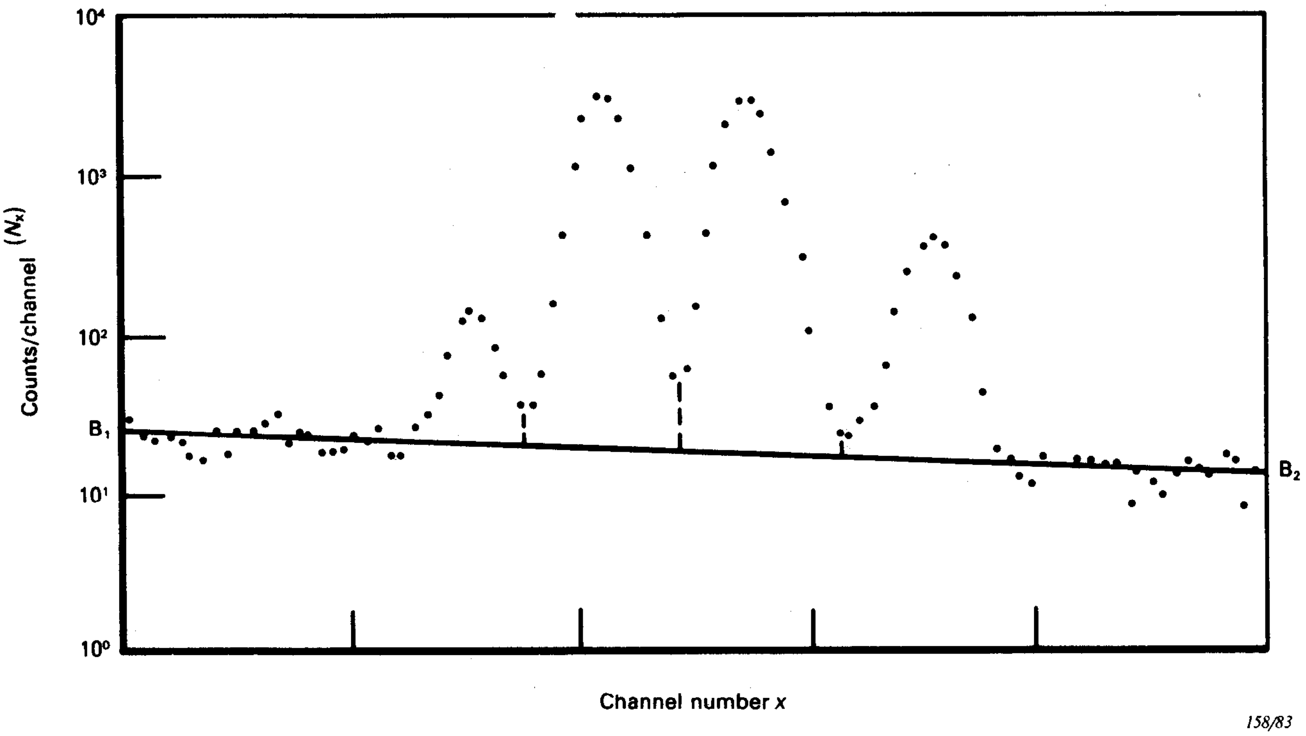

FIG. 18. — Background subtraction and peak area measurements.

Bureau of Indian Standards

BIS is a statutory institution established under the *Bureau of Indian Standards Act, 1986* to promote harmonious development of the activities of standardization, marking and quality certification of goods and attending to connected matters in the country.

Copyright

BIS has the copyright of all its publications. No part of these publications may be reproduced in any form without the prior permission in writing of BIS. This does not preclude the free use, in the course of implementing the standard, of necessary details, such as symbols and sizes, type or grade designations. Enquiries relating to copyright be addressed to the Director (Publications), BIS.

Revision of Indian Standards

Indian Standards are reviewed periodically and revised, when necessary and amendments, if any, are issued from time to time. Users of Indian Standards should ascertain that they are in possession of the latest amendments or edition. Comments on this Indian Standard may be sent to BIS giving the following reference :

Doc : No. LTDC 26 (1249)

Amendments Issued Since Publication

Amend No.	Date of Issue	Text Affected

BUREAU OF INDIAN STANDARDS

Headquarters:

Manak Bhavan, 9 Bahadur Shah Zafar Marg, New Delhi 110002
Telephones : 331 01 31, 331 13 75
Telegrams : Manaksanstha
(Common to all Offices)

Regional Offices:	Telephone
Central : Manak Bhavan, 9 Bahadur Shah Zafar Marg NEW DELHI 110002	331 01 31 331 13 75
Eastern : 1/14 C. I. T. Scheme VII M, V. I. P. Road, Maniktola CALCUTTA 700054	36 24 99
Northern : SCO 445-446, Sector 35-C, CHANDIGARH 160036	2 18 43 3 16 41
Southern : C. I. T. Campus, IV Cross Road, MADRAS 600113	41 24 42 41 25 19 41 29 16
Western : Manakalaya, E9 MIDC, Marol, Andheri (East) BOMBAY 400093	6 32 92 95

Branches : AHMADABAD. BANGALORE. BHOPAL. BHUBANESHWAR.
GUWAHATI. HYDERABAD. JAIPUR. KANPUR. PATNA.
TRIVANDRUM.

Printed at Printograph, Delhi, India